IKR Publishers

IKR Journal of Engineering and Technology (IKRJET)
Journal homepage: https://ikrpublishers.com/ikrjet/
Volume-2, Issue-4 (July-August) 2026
OPEN ACCESS
ISSN: 3107-7331 (Online)

Jarosite Formation as an Iron-Precipitation Route in Hydrometallurgy: Process Chemistry, Kinetics, Impurity Deportment, Solid–Liquid Separation, and Residue Sustainability—A Critical Review

Antonio Clareti Pereira, PhD*
PhD in Chemical Engineering University of São Paulo (USP) Belo Horizonte, Minas Gerais, Brazil

DOI:*10.5281/zenodo.21969803*

ARTICLE INFO

Article history:
Received : 02-08-2026
Accepted : 11-08-2026
Available online : 16-08-2026

Citation: Pereira, A. C. (2026). Jarosite Formation as an Iron-Precipitation Route in Hydrometallurgy: Process Chemistry, Kinetics, Impurity Deportment, Solid–Liquid Separation, and Residue Sustainability—A Critical Review. *IKR Journal of Engineering and Technology (IKRJET), 2*(4), 89-112.

ABSTRACT **Original Research Article**

Jarosite precipitation remains an important route for removing ferric iron and incorporating sulfate into the precipitate in acidic hydrometallurgical liquors, yet process performance is often judged solely by iron removal. This structured critical narrative review evaluates jarosite as a coupled reaction–particle engineering–separation–residue system. The updated bibliography contains 102 references: 99 scientific sources used in the synthesis, two methodological sources, and one earlier authorial review retained only for transparent positioning of novelty. A documented literature update through 8 August 2026 adds recent evidence on integrated Fe–Pb–Zn recovery, selective Pb extraction, and indium recovery from industrial jarosite. Quantitative synthesis shows that operating windows and kinetic parameters are strongly system-dependent: reported examples range from industrial jarosite precipitation near 90–95 °C to low-temperature continuous precipitation, while apparent activation energies around 42–44 kJ mol−1 recur in selected crystallization/dissolution studies but do not establish a universal mechanism. Selectivity must be evaluated jointly with residual Fe, valuable-metal loss, particle size, filtration behavior, cake moisture, and residue stability. The revised six-gate framework therefore requires measurable evidence at each decision stage rather than a single Fe-removal target. The review identifies persistent gaps in high-ionic-strength thermodynamic modeling, standardized kinetic reporting, quantitative solid–liquid separation data, continuous pilot validation, closed mass balances, and integrated techno-economic/life-cycle assessment.

Keywords: Jarosite Precipitation, Iron Removal, Hydrometallurgy, Impurity Deportment, Solid–Liquid Separation, Residue Valorization.

Highlights

- Jarosite performance must be evaluated beyond ferric-iron removal alone.
- A-site species, acidity, sulfate, seeding, mixing, and ageing jointly control particle quality.
- Impurity retention can support detoxification but also cause valuable-metal losses.
- Process selection should couple precipitation performance with residue stability and circularity.

Graphical Abstract

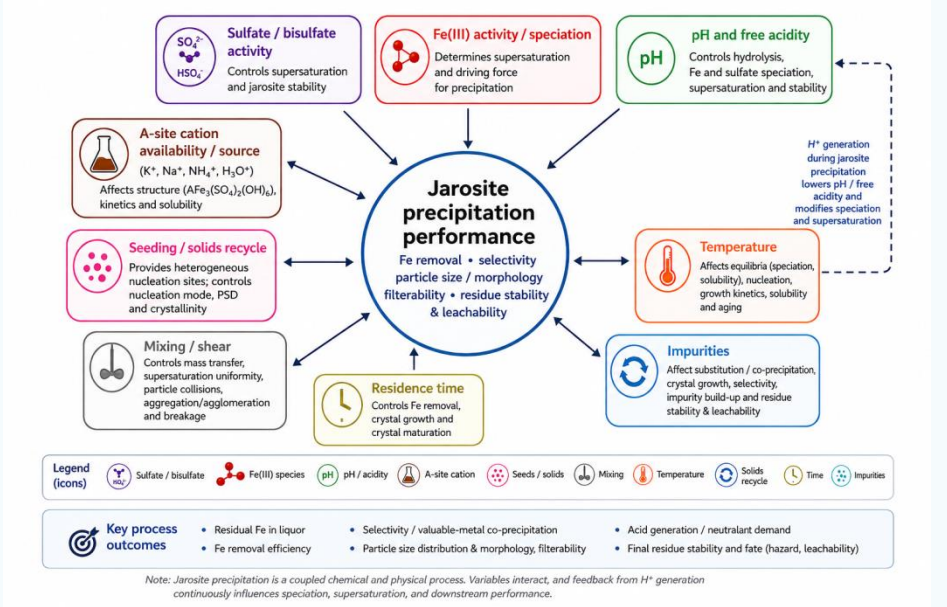

*Corresponding author: Antonio Clareti Pereira, PhD
PhD in Chemical Engineering University of São Paulo (USP) Belo Horizonte, Minas Gerais, Brazil

Introduction

Iron as an impurity in hydrometallurgical circuits

Iron enters hydrometallurgical liquors through dissolution of iron-bearing gangue, oxidation of sulfides, pressure or atmospheric leaching, and recycling of secondary materials. Once present as Fe(III), it can increase neutralization demand, compete for ligands or extractants, promote scale or secondary precipitation, and contaminate downstream products. Jarosite precipitation became important because it can remove ferric iron under acidic sulfate conditions while producing a crystalline solid that is, in many circuits, easier to separate than amorphous ferric hydroxides. Its historical importance is especially clear in zinc hydrometallurgy, but recent work also connects jarosite chemistry with copper, nickel, secondary-zinc, recycling, and waste-treatment circuits (Dutrizac & Jambor, 2000; Höber & Steinlechner, 2021; Qin et al., 2020; Thibault et al., 2020; Wang et al., 2021; X. Zhou et al., 2024).

Why a critical process review is needed

A removal-efficiency-only assessment overlooks that precipitation affects both liquor and solids. Maximizing Fe removal can also boost acid use, trap metals, produce finer particles, increase moisture, or create hard-to-stabilize residues. Recent studies view jarosite as a combined reaction–separation–residue issue, not just a single precipitation. Literature shows jarosite acts as impurity scavenger, oxyanion carrier, temporary host, or precursor for further processing. These roles explain why similar iron-removal results can yield different plant outcomes.

Scope, novelty, and review questions

This review focuses on jarosite formation as an iron-precipitation route and treats downstream residue processing as a consequence of the composition and structure created during precipitation. It asks five linked questions: (i) which chemical and kinetic conditions favor selective jarosite formation; (ii) how do operating variables control nucleation, growth, aggregation, and ageing; (iii) how are valuable and hazardous elements deported to the solid; (iv) which precipitate properties govern settling, filtration, washing, and handling; and (v) when is jarosite preferable to alternative iron-removal routes once residue stability and circularity are included. The present contribution is deliberately process-engineering oriented and emphasizes quantitative comparability, industrial transferability, and measurable decision criteria.

Positioning relative to previous jarosite reviews

A specific novelty check is necessary because the literature already contains authoritative reviews on jarosite mineralogy, iron-precipitation residues, formation/dissolution, environmental behavior, and residue reutilization. The author's 2026 structured review is also close in topic. The present manuscript therefore retains that publication explicitly for positioning rather than using it as evidence, and differentiates itself through updated August 2026 coverage, quantitative operating and kinetic synthesis, explicit solid–liquid-separation evidence, and an operational six-gate decision framework.

Table 1. Positioning of the present review relative to previous jarosite reviews

Review	Main emphasis	Quantitative / separation focus	Differentiation of present review
Dutrizac & Jambor (2000)	Foundational mineralogy and hydrometallurgical application	Foundational chemistry; limited modern quantitative/separation audit	Current evidence + quantitative process/separation synthesis
Höber & Steinlechner (2021)	Iron-precipitation residue processing	Route comparison; separation not central	Links precipitation quality to residue processing
Cruells & Roca (2022)	Formation, structure, reactivity, environment	Mechanistic; separation not central	Adds operating, kinetic and decision tables
Singh et al. (2023).	Residual-metal recovery	Recovery centered	Places recovery downstream of precipitation/selectivity decisions
Buriti et al. (2024).	Precipitation/dissolution state of the art	Strong chemistry/kinetics; separation not central	Adds industrial transferability and separation evidence
Chen et al. (2025).	Detoxification/reutilization	Treatment centered	Adds upstream process–particle linkage and maturity appraisal
Pereira (2026)	Broad 2020–2025 structured jarosite review	Broad synthesis; limited quantitative separation audit	Present review is narrower, updated to Aug 2026, quantitatively process-centered
Present review	Reaction–particle–separation–residue system	Quantitative operating/kinetic/selectivity/separation evidence	Measurable six-gate framework + industrial-transferability focus

Note. Author's comparative synthesis based on the cited reviews. "NR" or limited coverage should not be interpreted as a criticism of a review whose scope was different.

This comparison is central to the revised novelty claim. The present paper does not claim novelty in covering jarosite per se; novelty is claimed in the integrated, more quantitative process boundary, the explicit separation-evidence audit, the updated 2026 residue-recovery literature, and the operationalization of decision gates. A formal similarity check against Pereira (2026) is still recommended before submission.

Figure 1 is included here to position jarosite precipitation within the complete purification–separation–residue chain. The revised figure removes the crowded "process objective" overlay and distinguishes A-site species from those introduced by external reagent addition.

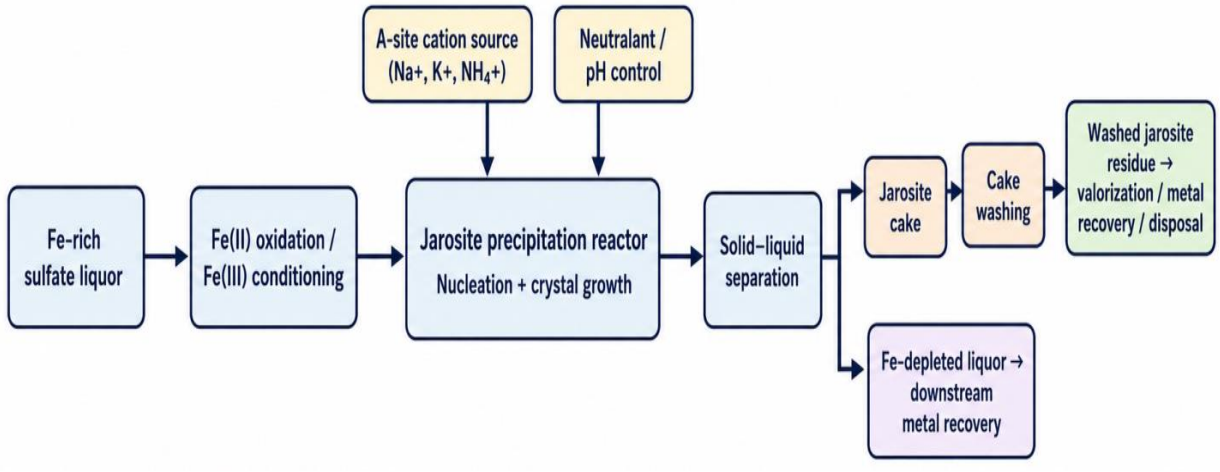

Figure 1. Conceptual flowsheet of iron removal through jarosite precipitation

Note. Author's conceptual synthesis informed by Dutrizac and Jambor (2000), Asimi et al. (2020), Cruells and Roca (2022), and the process-integration evidence reviewed here.

The flowsheet makes the system boundary explicit: a condition that improves precipitation but degrades washing, valuable-metal recovery, or residue fate is not automatically an overall process improvement.

Review Methodology and Evidence Appraisal

Review design and corpus boundary

The work was conducted as a structured critical narrative review rather than a systematic review or meta-analysis. The legacy discovery-stage hit lists, complete exports, duplicate-removal logs, and screened-result counts were not preserved and are therefore not reconstructed or estimated. To strengthen auditability, the revision adds a documented update search completed on 8 August 2026 and records the exact search families, sources, inclusion logic, and newly included records. The final bibliography contains 102 references: 99 scientific sources used in the synthesis, two methodological sources (Aromataris & Munn, 2020; Page et al., 2021), and Pereira (2026), which is retained only to position novelty and is not used as evidence for scientific conclusions.

Search reconstruction and eligibility logic

The legacy audit indicates that Google Scholar and publisher searches were previously screened for duplication, relevance, publication type, and temporal eligibility. For the present revision, an update search was run through scholarly web indexing and publisher platforms using four pre-specified families: (1) "jarosite precipitation" AND (iron removal OR hydrometallurgy); (2) jarosite AND (kinetics OR nucleation OR growth OR crystallization); (3) "jarosite residue" AND (recovery OR valorization OR reduction roasting OR leaching); and (4) jarosite AND (filtration OR settling OR "particle size" OR "solid–liquid separation"). Searches were limited to peer-reviewed records available through 8 August 2026, followed by title/abstract screening and publisher-page metadata verification. This update added four directly relevant 2026 studies and two foundational 2014 continuous-precipitation studies needed for quantitative separation/process evidence. Because the original legacy hit counts remain unavailable, no PRISMA flow count is fabricated.

Critical appraisal fields

For the revision, extraction fields were expanded to include: solution/feed type; initial and final Fe chemistry; sulfate/free-acidity information; A-site species or external reagent where applicable; temperature; residence time; seeding and mixing; Fe removal or precipitation; valuable-metal loss/selectivity; phase identification; particle-size descriptors; settling/filtration/washing metrics; kinetic model and reported parameters; experimental scale; mass-balance closure; uncertainty/replication; and downstream residue outcome. Missing quantities are retained as not reported (NR) rather than inferred. This policy is essential because the evidence base is heterogeneous and does not support direct meta-analysis.

Table 2 summarizes the revised review protocol and makes clear which elements are prospectively auditable and which legacy discovery details remain unavailable.

Table 2. Review design, updated search, corpus boundary, and critical-appraisal fields

Item	Implementation in this review
Review type	Structured critical narrative review with retrospective evidence appraisal; not claimed as a systematic review or meta-analysis.
Retained bibliography	95 references in the analytical bibliography; two 2026 authorial records in the working audit were treated as post-cutoff and excluded from the main synthesis.
Temporal boundary	Contemporary evidence concentrated in 2020–2025, with the foundational Dutrizac and Jambor (2000) review retained for historical/mechanistic context.
Documented discovery information	The available audit records were screened using Google Scholar for duplication, relevance, publication type, and temporal eligibility. Original hit lists and complete screening counts were not retained.
Eligibility logic	Jarosite precipitation/formation, iron removal, crystallization, impurity deportment, solid–liquid separation, dissolution/transformation, environmental stability, or residue treatment/valorization.
Critical appraisal fields	Solution type; feed/discharge chemistry; phase identification; temperature; acidity/pH; sulfate; residence time; seeding; mixing; impurity transfer; particle properties; separation data; uncertainty; industrial transferability.
Review-process limitation	Single-reviewer reconstruction and appraisal; no independent calibration or inter-rater reliability statistic.

Note. Author's synthesis based on the retained reference audit and methodological guidance from Aromataris and Munn (2020) and Page et al. (2021).

The table also separates evidence appraisal from a formal systematic-review quality score. This distinction prevents the retained bibliography from being presented with a level of

search reproducibility that the archived records do not support.

Evidence-map limitations

The updated evidence remains heterogeneous in solution chemistry, assay basis, residence-time definition, scale, and reporting completeness. This heterogeneity is treated as a result rather than hidden by a pooled average. Quantitative tables in Sections 4–11 therefore preserve system boundaries and explicitly mark NR fields. Continuous and industrially oriented precipitation evidence is much less abundant than laboratory mineralogical, transformation, and residue-treatment evidence; the revised discussion consequently separates mechanistic plausibility from industrial transferability.

Limitations of the review process

Searching, retrospective coding, and interpretation were conducted without an independently calibrated second reviewer, so no inter-rater reliability statistic is reported. The revised update search improves currency and transparency but cannot recover legacy hit lists or historical screening counts. The manuscript should therefore be read as an auditable structured critical narrative synthesis, not as proof that every eligible publication has been captured. A final Scopus/Web of Science rerun with saved exports is recommended before Q1 submission if subscription access is available.

Chemistry, Crystallography, Stoichiometry, and Process-Chemistry Constraints

Jarosite-type structure and compositional flexibility

Jarosite-group phases are commonly represented by the idealized formula $AFe_3(SO_4)_2(OH)_6$, where the A site can be occupied by monovalent species such as K^+, Na^+, NH_4^+, or H_3O^+. This formula is useful for process stoichiometry, but natural, synthetic, and industrial jarosites can deviate from ideality due to vacancies, mixed A-site occupancy, Fe-site substitution, anion substitution, surface adsorption, and secondary-phase association. The mineralogical literature therefore cautions against equating a nominal "jarosite" XRD pattern with a single chemically ideal phase (Cruells & Roca, 2022; Dutrizac & Jambor, 2000; Grigg, Notini, et al., 2024; Hu et al., 2025; Peng, He, et al., 2023; Shi et al., 2022; Shi et al., 2023). Aluminum substitution, lead-bearing variants, and oxyanion-bearing solids demonstrate that apparently small compositional changes can alter stability, surface reactivity, and contaminant retention (Grigg, Notini, et al., 2024; Hu et al., 2025; Peng, He, et al., 2023; Shi et al., 2022).

Figure 2 is inserted at this point because structural flexibility is the basis for both useful contaminant capture and unwanted valuable-metal loss.

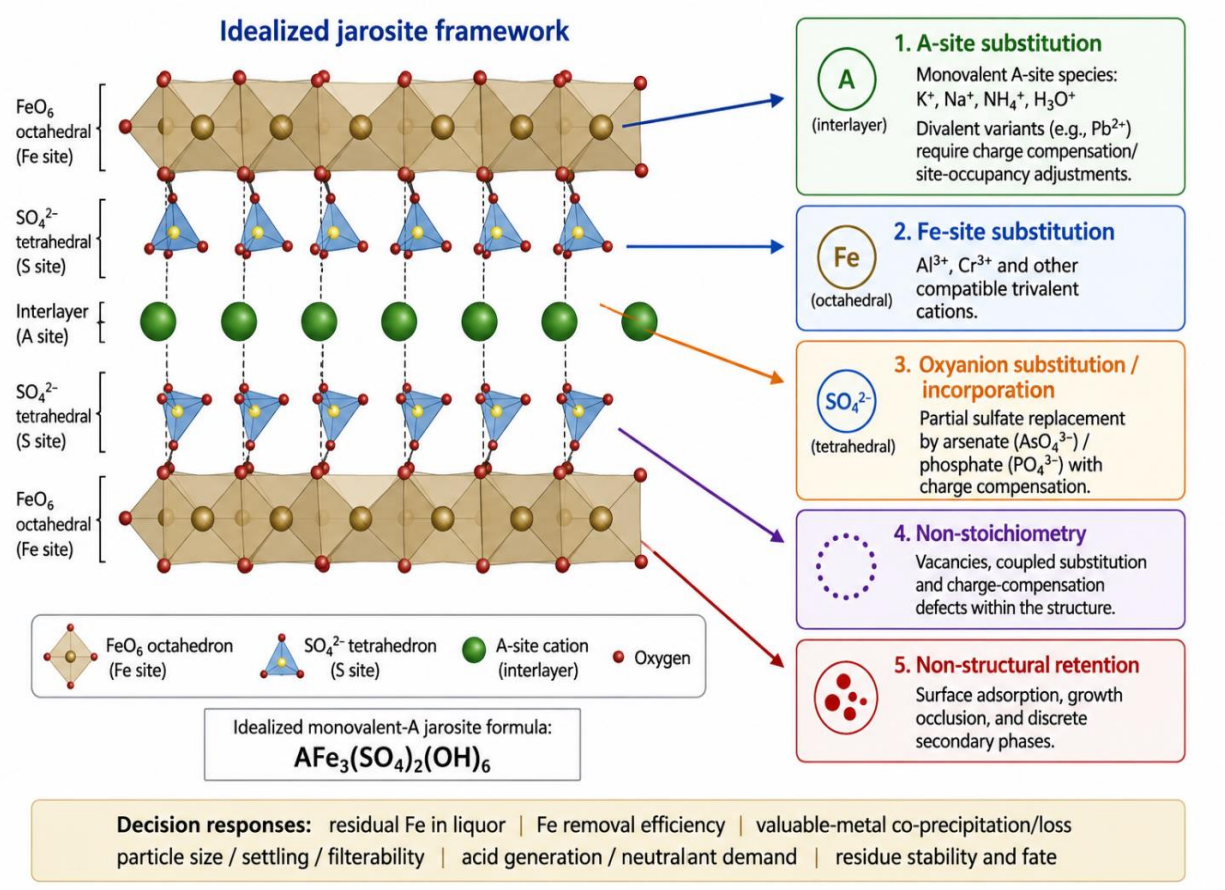

Figure 2. Idealized jarosite framework and principal substitution/retention mechanisms

Note. Author's conceptual synthesis informed by Dutrizac and Jambor (2000), Cruells and Roca (2022), Grigg, Notini, et al. (2024), Hu et al. (2025), and Shi et al. (2022, 2023).

The structural view reinforces a key analytical rule used throughout this review: bulk solid composition alone cannot distinguish lattice substitution from adsorption, occlusion, or the presence of associated secondary phases.

Idealized precipitation stoichiometry and acid generation

For a monovalent A-site cation, an idealized precipitation reaction can be written as:

$$A^+ + 3Fe^{3+} + 2SO_4^{2-} + 6H_2O \rightarrow AFe_3(SO_4)_2(OH)_6(s) + 6H^+.$$

This equation highlights a process feature that is sometimes obscured when only iron removal is reported: jarosite formation generates acidity. Maintaining a productive supersaturation therefore requires coupling iron hydrolysis with controlled neutralization, suitable A-site-ion activity, and adequate sulfate availability. The practical demand for neutralization depends on solution speciation, free acidity, reagent chemistry, competing precipitation, dilution, and the non-ideal composition of the solid. Consequently, stoichiometric acid generation is a starting point for process design rather than a complete reagent balance.

Ferric-sulfate speciation, hydrolysis, and supersaturation

Jarosite precipitation occurs in concentrated acidic sulfate media in which activity coefficients depart substantially from unity. Fe(III) is distributed among free, hydrolyzed, and sulfate-complexed species, so concentration is not equivalent to chemical activity. Measured pH is likewise not interchangeable with free acidity or proton activity. The retained literature uses thermodynamic diagrams and speciation arguments to define feasible conditions, but it does not provide a sufficiently harmonized set of high-ionic-strength parameters for a universal predictive model. For this reason, the revised title uses "Process Chemistry" rather than overclaiming a comprehensive thermodynamic synthesis. Future predictive work should explicitly document the activity model and database used, rather than transferring dilute-solution equilibrium constants directly to concentrated plant liquors (Buriti et al., 2024; Zhou et al., 2024).

Phase competition and non-equilibrium effects

Thermodynamic stability does not guarantee that the equilibrium phase forms on an industrial residence-time scale. Jarosite competes with poorly crystalline ferric precipitates, iron oxyhydroxides, schwertmannite-like phases, basic sulfates, and transformation products. Saturation index or predominance fields are therefore boundary conditions rather than kinetic predictions. Zhou et al. (2024) used an Eh–pH analysis for a K–S–Fe–H2O system to support selective iron removal, but the broader corpus rarely reports activity-model choice, ionic-strength sensitivity, or uncertainty in equilibrium constants. This reporting gap is itself a key result: high-ionic-strength process chemistry requires validated Pitzer/SIT/e-NRTL-type treatments or equivalent activity models, coupled to measured plant-liquor compositions, before universal stability maps are credible.

Nucleation, Growth, Aggregation, and Precipitation Kinetics

Mechanistic sequence

A mechanistic description of jarosite formation should distinguish at least five coupled stages: ferric-sulfate speciation and hydrolysis, generation of supersaturation, nucleation, crystal growth, and aggregation/ageing. Recent precipitation and crystallization studies reinforce that these stages are not independent. A condition that accelerates Fe removal can also increase nucleation density, alter morphology, or change crystallinity, thereby affecting subsequent separation performance (Asimi et al., 2020; Buriti et al., 2025b; Oladipo & Ojumu, 2023; Peng et al., 2024; Shi et al., 2023). Seeding changes the balance between homogeneous and heterogeneous nucleation, while mixing controls local reagent dispersion, concentration gradients, collision frequency, and breakage of weak aggregates.

Figure 3 is placed here to distinguish the temporal stages of formation from the operating variables that influence them.

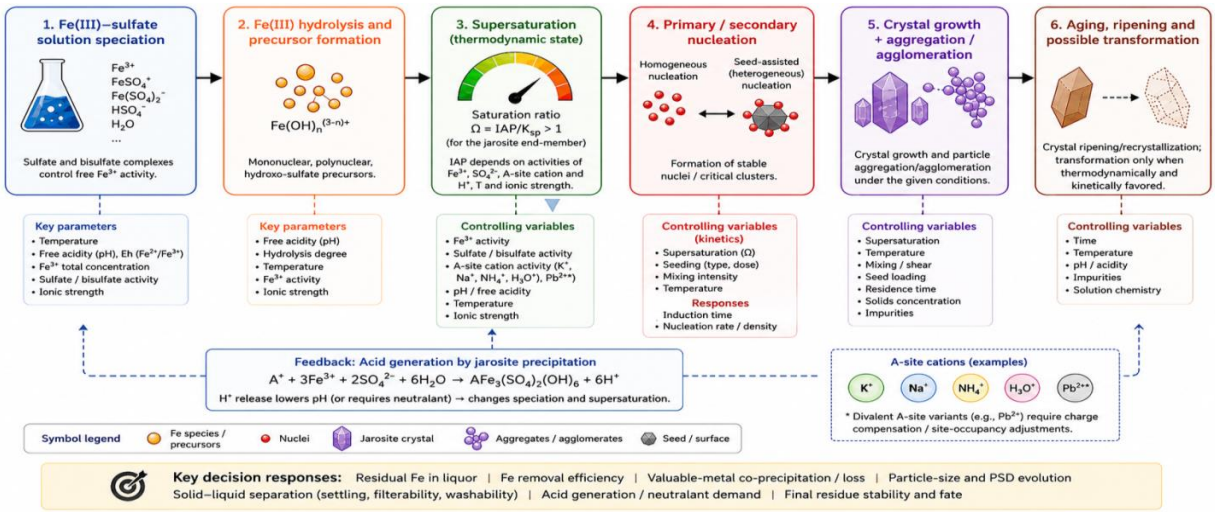

Figure 3. Mechanistic pathway from ferric-sulfate speciation to jarosite ageing and transformation

Note. Author's conceptual synthesis informed by Asimi et al. (2020), Buriti et al. (2024, 2025b), Oladipo and Ojumu (2023), and Peng et al. (2024).

The scheme is deliberately sequential but not strictly linear: nucleation, growth, aggregation, and transformation may overlap, especially when solids are recycled or the liquor composition evolves continuously.

Induction period and temperature dependence

The induction period indicates when a solution shifts from being supersaturated to crystals forming. Higher temperatures speed up hydrolysis and precipitation, but also alter morphology, aging, and dissolution (Buriti et al., 2025a; Buriti et al., 2025b; Islas et al., 2020; Trueman et al., 2020). Activation energies are relevant only within tested conditions. Caution is needed when applying results from dilute solutions to industrial liquors.

Kinetic-model interpretation

Kinetic studies cover precipitation, acid dissolution, leaching, and thermal transformation. Parameters aren't directly interchangeable but allow comparison of model form, activation energy, and validity range. High regression quality doesn't prove mechanism; the controlling step must align with phase changes, particle-area, induction, and transport. Table 3 reports parameters explicitly rather than discussing models qualitatively.

Table 3. Representative kinetic models and parameters reported for jarosite formation, dissolution, and transformation

Study/process	Conditions	Model/form	Reported parameter(s)	Interpretation/limitation
Zhou et al. (2024).— K-jarosite crystallization	95 °C optimum; 90 min; seed 10 g/L; pH 1.76, endpoint ≈3	Avrami crystallization	n ≈ 2.5; Ea = 42.68 kJ mol−1	Strong formation evidence for this liquor; not transferable without activity/composition match
Buriti et al. (2025b).— K-jarosite precipitation	296–343 K; variable K/Fe, seeding, agitation	Stage-wise precipitation behavior	Three stages at room temperature; K/Fe and T dominant; no universal Ea reported	Shows mechanism changes with T/composition; agitation/seeding not significant in tested window
Calla-Choque & Lapidus (2021). — industrial jarositedissolution	Acidic thiourea/oxalate media	Multi-particle shrinking-core	Ea ≈ 43–44 kJ mol−1	Heterogeneous-reaction control in tested range; dissolution parameter, not precipitation constant
Nolasco et al. (2025). — Ag extraction from jarosite residue	Acidic thiourea; up to 60 °C	Shrinking-core / surface reaction	kexp ≈ 1.1 min−1 at 60 °C in reported condition; Ag extraction up to ≈98%	Useful for downstream reactivity; cannot be used as jarosite-formation kinetics
Olcay et al. (2025).— thermal decomposition	Industrial sodium jarosite; staged heating	Solid-state kinetic analysis	Ea ≈ 22.32, 42.23, and 46.31 kJ mol−1 for successive stages	Multiple stages confirm that a single apparent Ea can conceal mechanism changes
Islas et al. (2020). — jarositedissolution	Multiple acidic/alkaline conditions	Shrinking-core framework	Mechanistic transition between reaction and mass-transfer influence; parameter is condition-dependent	Highlights sensitivity to particle size and solution chemistry

Note. Values are reported on the original study basis. Ea = apparent activation energy; NR = not reported. Formation, dissolution, and thermal decomposition constants must not be pooled as if they described a single mechanism.

The recurring apparent activation energies near 42–44 kJ mol−1 reported in selected studies are noteworthy but do not establish a universal controlling mechanism, as the studies address different reactions and solution/solid states. The revised discussion therefore treats kinetic parameters as local evidence with explicit validity windows.

Precipitation and dissolution as linked phenomena

The same structural features that determine precipitation kinetics influence subsequent dissolution or transformation. Acid decomposition, thiourea/oxalate leaching, biological

reduction, and Fe(II)-induced transformation all show that jarosite stability is dynamic rather than absolute (Buriti et al., 2025a; Calla-Choque & Lapidus, 2020; Calla-Choque & Lapidus, 2021; Chen et al., 2022; Chen et al., 2021; González et al., 2020; Jin et al., 2024; Jin et al., 2020; Yang et al., 2020). This has two implications for precipitation design. First, the process should not produce a solid whose downstream instability is incompatible with storage or washing conditions. Second, intentionally producing a more reactive jarosite may be beneficial if the residue is an intermediate feed for subsequent metal recovery.

Effects of Operating Variables and A-Site Species / Reagent Strategy

Temperature, acidity, and ferric concentration

Temperature, acidity, and Fe(III) concentration determine the available driving force for precipitation and the time required to reach a target residual iron concentration. Industrial and laboratory evidence shows that their effects are strongly coupled (Asimi et al., 2020; Buriti et al., 2025b; Oladipo & Ojumu, 2023; Peng et al., 2024; X. Zhou et al., 2024). Raising temperature may accelerate hydrolysis and growth, but it also changes evaporation, energy demand, corrosion exposure, and the stability of competing phases. Increasing the neutralization rate can locally increase supersaturation, which may favor rapid nucleation at the expense of coarser, more readily filterable particles. For process control, reagent addition strategy and local mixing are therefore as important as the bulk pH set point.

Sulfate activity and A-site species

The A-site species/reagent is not merely a stoichiometric additive. Sodium, potassium, ammonium, and hydronium jarosites differ in reagent requirements, solution inventory, downstream compatibility, cost, and potential effects on product properties. Direct technical-economic comparison of sodium and ammonium routes confirms that the preferred agent is circuit-specific rather than universal (AsimiNeisiani et al., 2023). Potassium-jarosite kinetic work likewise shows that composition and temperature affect formation rate, morphology, and crystallinity (Buriti et al., 2025b). Hydronium-bearing phases provide a useful limiting case where the solution chemistry itself supplies the A-site species, but they should not be assumed equivalent to alkali- or ammonium-containing products.

Seeding, ageing, solids recycle, and mixing

Seeding can shorten induction time and redirect supersaturation toward crystal growth, but recycled solids may also accumulate impurities or broaden the particle-size distribution. Ageing after Fe removal can improve crystal order and aggregation in some systems while increasing residence time and reactor volume. Mixing has a similarly non-monotonic role: insufficient mixing can produce local neutralization gradients, whereas excessive shear can disrupt weak agglomerates and increase fines. The retained literature on industrial-scale operation, biogenic precipitation, hydrothermal crystallization, and process iron balance supports treating these variables as an integrated particle-engineering problem rather than independent operating knobs (Asimi et al., 2020; Oladipo & Ojumu, 2023; Peng et al., 2024; Qin et al., 2020; Wang et al., 2021).

Table 4 consolidates representative operating windows and quantitative responses. The purpose is not to define a universal optimum, but to show the magnitude of cross-study heterogeneity and the need to retain feed chemistry and measurement basis.

Table 4. Selected quantitative operating windows for jarosite precipitation and iron removal

Study / system	Operating window or tested condition	Fe response	Selectivity / solid response	Process interpretation
Asimi et al. (2020).— industrial zinc JPP	≈90 °C; ≈300 min; pH ≈1; Na2SO4 ≈2 g/L; mixing ≈500–600 rpm	Plant-scale Fe precipitation ≈80%; ≈85% reported with zinc-calcine alkalinity in tested strategy	Low-contaminant jarosite target; strong sensitivity to operating parameters	Industrial evidence that "optimum" is a coupled plant condition, not one-factor maximum
Asimi Neisiani et al. (2023).— industrial precipitating-agent comparison	Alternative Na/NH4-based reagents under industrially relevant testing	Fe removal: NH4OH 90.85%; Na2CO3 84.31%; NH4HSO4 77.13%; NaHSO4 74.54%	Technical/economic ranking differs from Fe-removal ranking alone	Agent selection must include cost, downstream ions and solid handling
Zhou et al. (2024).— Co/Ni-bearing scrap leach liquor	95 °C; K2SO4 coefficient 1.5; seed 10 g/L; 90 min; pH 1.76, endpoint ≈3	Fe removal >99%	Co and Ni losses <2%; jarosite particles ≈0.2–5.0 μm	Strong example of simultaneous Fe target + selectivity + particle characterization
Buriti et al. (2025b).— K-jarosite	296–343 K; variable K/Fe ratio, agitation and seeding	Rate increased with T and K/Fe in tested range	Higher T and K/Fe improved crystallinity/crystallite size; seeding/agitation not significant	Demonstrates non-universality of assumed seeding/mixing effects
Kaksonen et al. (2014a,b) — continuous two-stage CSTR	Ambient T; influent pH 1.0–2.2; continuous operation	Fe2+ oxidation 96–99%; Fe precipitation 8.2–54% depending on pH	Cu removal 0.25–2.5%; Ni 0.01–0.26%; precipitates 75–99% jarosite with good settling/filterability	Rare continuous evidence linking chemistry, selectivity and separability

Note. Values are retained on the original study basis; they are not normalized across different feed chemistries. NR indicates not reported. The table is intended to display heterogeneity, not support a pooled optimum.

The cross-coupling shown in Table 3 explains why one-factor optimization is unreliable. For example, a change intended to increase Fe conversion can simultaneously alter supersaturation, nucleation density, aggregation, and impurity retention.

Impurity loading as an operating variable

Industrial liquors contain elements that can alter nucleation surfaces, substitute into the structure, sorb to newly formed solids, or precipitate independently. Lead-bearing jarosite growth on anglesite, Pb substitution in natrojarosite, and Ga/In enrichment during precipitation show that impurity inventory can change both kinetics and the meaning of "selective" iron removal (Dong et al., 2025; Hu et al., 2025; Shi et al., 2023; Sun et al., 2025). Process optimization should therefore include the feed impurity fingerprint as a state variable, not merely as a post-precipitation assay.

Figure 4 is inserted after the operating-variable discussion to visualize this coupled control problem.

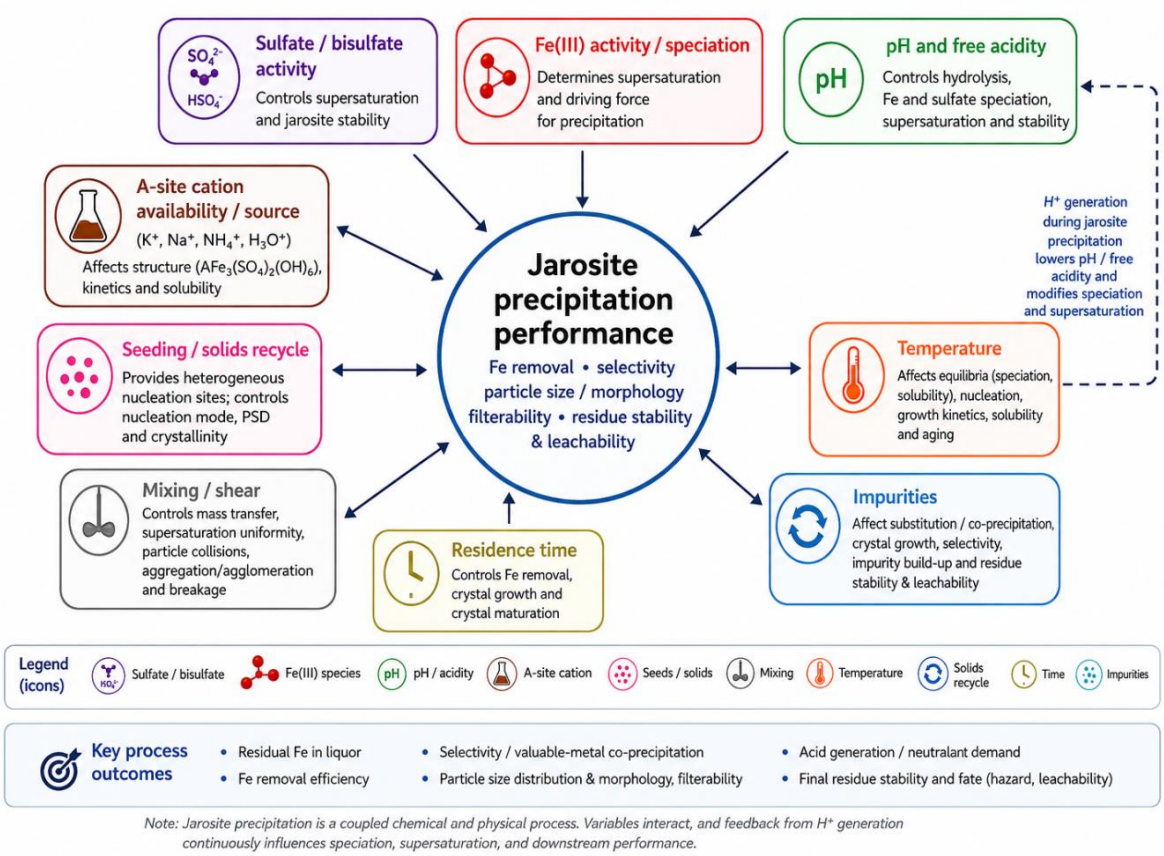

Figure 4. Interaction network of the main variables governing jarosite precipitation performance

Note. Author's conceptual synthesis based on the operating-variable framework developed in this review.

The network is not a calibrated causal model. It is a process map intended to guide experimental design, emphasizing that the same output—such as residual Fe—can result from different combinations of chemistry, hydrodynamics, and solids history.

Impurity Deportment, Selectivity, and Valuable-Metal Losses

Mechanisms of impurity retention

Impurity transfer to jarosite can occur through several mechanisms that are analytically distinct but operationally simultaneous: crystallographic substitution, surface adsorption, co-sorption, occlusion during growth, retention of pore solution, entrainment of fine secondary solids, and precipitation of discrete impurity-bearing phases. Spectroscopic and microstructural studies on As, Sb, Pb, and substituted jarosites demonstrate that a single bulk assay cannot identify the responsible mechanism (Hu et al., 2025; Karimian et al., 2023; Shi et al., 2022; Shi et al., 2023). Mechanistic assignment matters because structural incorporation, surface adsorption, and trapped solution respond differently to washing, pH changes, ageing, and later leaching.

Figure 5 is inserted here to separate the principal impurity-retention mechanisms before the element-specific discussion.

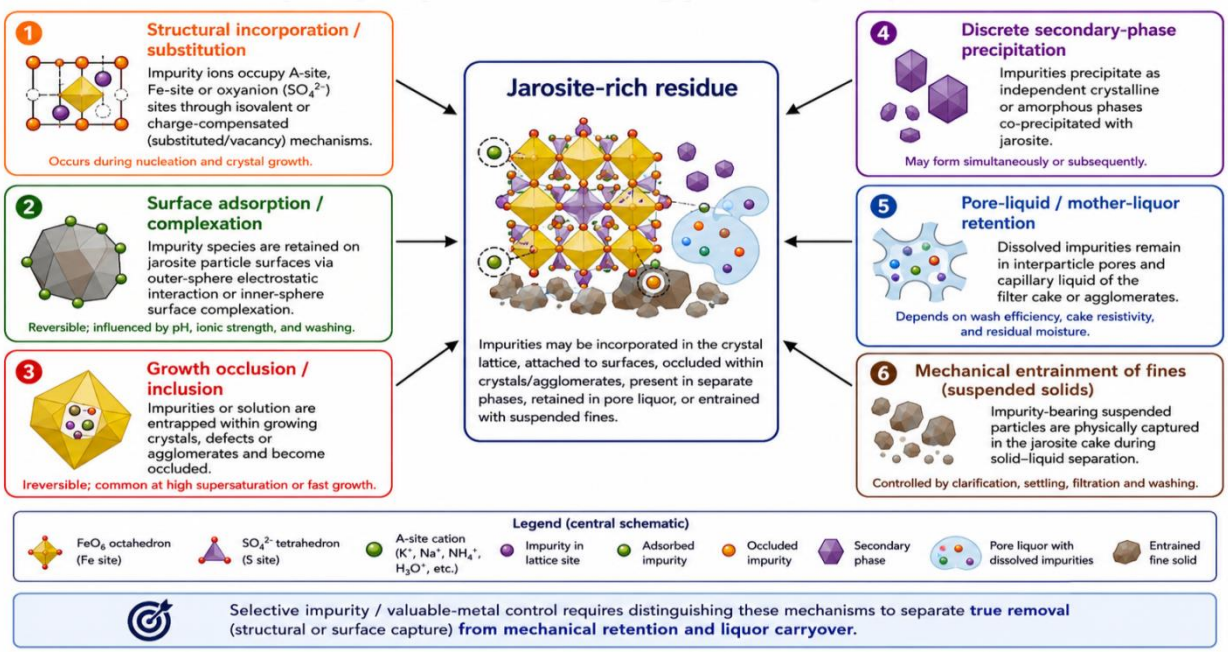

Figure 5. Mechanisms of impurity deportment to jarosite-bearing solids

Note. Author's conceptual synthesis informed by Karimian et al. (2023), Hu et al. (2025), Shi et al. (2022, 2023), Jin et al. (2023, 2024), and related transformation studies.

The figure highlights why washing tests and phase-resolved characterization are indispensable: retained pore liquor, surface adsorption, and structural substitution can produce similar bulk assays but very different process and environmental behavior.

Table 5 presents the revised impurity discussion as quantitative/selectivity evidence, as reported in the original studies. Missing quantities are shown explicitly rather than replaced by qualitative ranking.

Table 5. Quantitative impurity deportment and selectivity evidence in representative jarosite systems

Study/material	Quantitative response	Mechanistic evidence	Selectivity interpretation	Transferability
Zhou et al. (2024) — Co/Ni-bearing sulfate liquor	Fe removal >99%; Co and Ni losses <2%	Jarosite phase confirmed by XRD/SEM-EDS; particle size ≈0.2–5 µm	Demonstrates Fe selectivity must be expressed together with valuable-metal loss	Laboratory/bench process evidence on real scrap-derived liquor
Kaksonen et al. (2014a,b) — continuous Fe/Cu/Ni liquor	Fe in precipitate 29.2–34.0 wt%; Cu 0.044–0.15 wt%; Ni 0.002–0.016 wt%; influent Cu/Ni precipitation losses low	75–99% jarosite; continuous CSTR	Low Cu/Ni co-precipitation at lower pH illustrates process-selectivity window	Continuous laboratory-scale CSTR; strong scale-up relevance
Dong et al. (2025) — Zn-leach precipitation	Ga/In occurrence state changes with jarosite precipitation; comparable universal fraction NR	Occurrence/dependence on jarosite phase examined	Valuable-element enrichment can be a loss or recovery opportunity depending on downstream route	Mechanistic/process evidence; mass-basis harmonization needed
Calla-Choque & Zárate-Silva (2026). — industrialjarosite	In recovery up to ≈98% at pH 8 with phosphate/pyrophosphate; Fe in solution ≈0.7% in reported condition	Selective alkaline complexation; phosphate stabilizes system	Shows downstream selectivity can be engineered rather than accepting bulk dissolution	Real industrial jarosite; laboratory recovery step
Yu et al. (2026). — Pb-bearing industrial jarosite	Pb/Fe selectivity 14.74; Pb extraction 74.6%; ≈14-fold selectivity improvement vs conventional acid leaching	Calcination–quenching lattice relaxation; oxygen defects lower Pb migration barrier ≈35%	Demonstrates kinetic control can separate toxic/valuable metals from Fe host	Real jarosite residue; advanced mechanistic characterization
Sun et al. (2025). — lead-jarosite precipitation	Element-specific Zn/Cu/In behavior reported; harmonized cross-study fraction NR	Precipitation/deportment dependent on phase path	Bulk Fe removal alone cannot represent valuable-metal retention	Relevant to Zn hydrometallurgy; quantitative basis must be retained study-by-study

Note. Author's synthesis based on the cited structural, spectroscopic, leaching, and transformation studies.

The table should be used as a diagnostic sequence rather than as mutually exclusive categories because several mechanisms can operate simultaneously in one industrial precipitate.

Arsenic and antimony

Arsenic behavior is among the best documented examples of the dual role of jarosite. Formation and transformation studies show that jarosite can immobilize arsenate under some conditions, yet reductive dissolution or mineral transformation can remobilize it (Burton et al., 2021; Gao et al., 2021; Jin et al., 2024; Jin et al., 2023; Jin et al., 2020; Karimian et al., 2023; Lee et al., 2025; Tang et al., 2020; Zhang et al., 2025). Phosphate, organic ligands, lead, and the presence of Fe(II) can modify this behavior (Gao et al., 2020; Jin et al., 2024; Jin et al., 2020; Zhang et al., 2025). Antimony can partition differently from arsenic during transformation, reinforcing the need to avoid treating all oxyanions as equivalent (Jin et al., 2023; Karimian et al., 2023).

Lead and other structural or co-precipitated elements

Lead can participate in jarosite-family solids through substitution, coprecipitation, nucleation on lead-bearing phases, or association with discrete phases. Lead-bearing jarosite synthesis and dissolution studies show that Pb retention can suppress mobility under one set of conditions yet create a metal-bearing residue requiring deliberate management under another (Hu et al., 2025; Peng, He, et al., 2023; Ryu & Kim, 2022; Shi et al., 2022; Shi et al., 2023). Similar logic applies to Cd, Cr, and other hazardous elements: high removal from solution may be beneficial for liquor purification but transfers environmental responsibility to the precipitate.

Valuable metals and selectivity

For valuable metals, the relevant metric is not removal from the liquor but loss from the recoverable circuit. Ga, In, Cu, Zn, Ag, and other elements may be enriched in jarosite-bearing residues by structural association, sorption, pore-liquid retention, or formation of separate phases (Conić et al., 2024; De-la-Cruz-Moreno et al., 2021; Dong et al., 2025; Janošević et al., 2023; Nolasco et al., 2025; Sun et al., 2025). The literature on Ga/In occurrence during precipitation and on lead-jarosite precipitation explicitly shows that the deportment of valuable elements varies with the precipitation pathway (Dong et al., 2025; Sun et al., 2025). A robust operating target should therefore report both residual Fe and recoverable-metal loss on a reconciled mass basis.

Selectivity as a multi-response criterion

A jarosite condition should not be classified as optimal solely because it removes a large fraction of Fe. A technically stronger criterion requires: adequate Fe removal; acceptable loss of valuable metals; controlled capture of hazardous species; a phase assemblage compatible with washing and storage; and a residue composition that does not preclude later recovery or valorization. This reframing converts impurity deportment from a side observation into a core process-design variable.

Precipitate Characterization and Solid–Liquid Separation

Why solid quality is a primary process response

A jarosite process produces two products: a treated liquor and a solid. The second product is often under-characterized even though its morphology, size distribution, crystallinity, porosity, impurity loading, and retained solution directly affect thickening, filtration, washing, transport, storage, and subsequent treatment. Recent kinetic and physicochemical studies show that the conditions that determine Fe conversion also alter crystal habit and solid properties (Buriti et al., 2025b; Oladipo & Ojumu, 2023; Peng, He, et al., 2023; Peng, Liu, et al., 2023). Consequently, characterization should be designed to link mineralogy to separation performance rather than to confirm phase identity alone.

Mineralogical and chemical characterization

At minimum, phase identification should distinguish jarosite from ferric hydroxides, iron oxyhydroxides, schwertmannite-like phases, gypsum, anglesite, and impurity-rich secondary phases. X-ray diffraction is most informative when combined with bulk chemistry and, where needed, microscopy, spectroscopy, thermal analysis, or element-specific methods. Studies on Pb substitution, Pb/As retention, and arsenic/antimony co-sorption show why phase identity and local chemical environment cannot be inferred from bulk composition alone (Hu et al., 2025; Karimian et al., 2023; Peng, He, et al., 2023; Shi et al., 2022). Rietveld analysis, SEM–EDS mapping, XPS, XAS, Raman/FTIR, and thermal analysis are therefore complementary rather than interchangeable.

Particle size, aggregation, and sedimentation

Particle-size distribution should distinguish primary crystallites from aggregates and should report the dispersion protocol used during measurement. Aggregation can be desirable when it produces robust particles that settle and filter rapidly, but fragile agglomerates may break under pumping or cake compression. Work on potassium-jarosite formation, industrial-scale precipitation, and the transformation of jarosite-bearing solids supports a direct link between synthesis conditions and aggregate structure (Asimi et al., 2020; Buriti et al., 2025b; Mombelli et al., 2021). This linkage is important for scale-up because a laboratory product that settles well in a quiescent cylinder may not retain the same structure after agitation, transfer, and filtration.

Continuous two-stage precipitation work provides rare process-relevant evidence that jarosite precipitates can show good settling and filterability while maintaining low Cu/Ni co-precipitation (Kaksonen et al., 2014a, 2014b).

Filtration, washing, and cake quality

Useful separation metrics include settling velocity, underflow solids concentration, filtrate flux, specific cake resistance, cake compressibility, residual moisture, washing efficiency, and dissolved-metal recovery from the pore liquor. The retained corpus contains far fewer quantitative filtration datasets than mineralogical or leaching studies, which is itself a significant evidence gap. In practice, washing performance can strongly affect apparent impurity content because pore-liquid entrainment can be mistaken for structural incorporation. Reporting washed and unwashed solid assay results, together with wash-water balance, would materially improve comparability across studies.

Table 6 summarizes the separation-related descriptors that can be verified in representative studies. The prevalence of NR entries is itself evidence: particle characterization is more common than filtration resistance, cake moisture, or washing efficiency.

Table 6. Reported solid–liquid-separation descriptors in representative jarosite studies

Study / evidence	Particle-size descriptor	Settling / filtration	Moisture/washing	What can be concluded
Zhou et al. (2024).	Jarosite particles ≈0.2–5.0 µm	NR	NR	PSD quantified, but equipment-scale separability cannot be inferred from PSD alone
Calla-Choque & Lapidus (2021).	Industrial natrojarosite: mean ≈10.26 µm; d80 ≈24 µm	NR in kinetic dissolution study	NR	Useful industrial-residue PSD descriptor; not a filtration dataset
Kaksonen et al. (2014b).	Phase/precipitate characterization; jarosite 75–99%	Reported good filterability and settling characteristics; numeric flux/resistance NR	NR	Rare continuous-process evidence linking jarosite phase quality to separability, but key equipment metrics remain unreported
Asimi et al. (2020)	Morphology/industrial low-contaminant product characterized; comparable D10/D50/D90 NR	Industrial operation; standardized filtration resistance NR	NR	Industrial relevance is high, yet common separation metrics needed for cross-study design are absent
Buriti et al. (2025b)	Crystallite size/crystallinity increase with T and K/Fe; harmonized PSD NR	NR	NR	Shows particle-quality response, but does not close the filtration-design gap

Note. Author's synthesis based on the particle-quality framework in this review and the characterization evidence cited in Sections 3–7.

The quantitative audit confirms that the title-level emphasis on solid–liquid separation is justified primarily as a documented evidence gap rather than as a mature, harmonized database. The retained examples provide PSD or qualitative settling/filterability information, but standardized filtrate flux, specific cake resistance, compressibility, residual moisture, and wash efficiency are rarely available together. Future studies should report these metrics on the same washed/unwashed mass basis used for impurity balances.

Industrial Applications and Flowsheet Integration

Zinc hydrometallurgy

Jarosite precipitation is most closely associated with zinc hydrometallurgy, in which iron management is integrated into leaching, solution purification, and residue handling. The retained literature includes industrial-scale precipitation, purification of leach solutions derived from electric arc furnace dust, zinc residue processing, and multiple residue recovery studies (Asimi et al., 2020; Hazaveh et al., 2020; Höber & Steinlechner, 2021; Rämä et al., 2023). These studies underline a central flowsheet point: the precipitation reactor cannot be optimized independently from the upstream Fe loading and the downstream value of metals remaining in solution or transferred to the residue.

Copper and bioleaching circuits

Jarosite can be either deliberate or detrimental in copper processing. In heap bioleaching, jarosite precipitation affects the iron balance and therefore the availability of ferric oxidant, acid consumption, and pore-space behavior (Wang et al., 2021). In other copper-bearing systems, jarosite residues become secondary resources containing Pb, Ag, Cu, Zn, or In that may warrant dedicated treatment (Conić et al., 2024; Janošević et al., 2023; Kamberović et al., 2021). The process implication is that precipitation should be managed against the entire iron–sulfur–metal balance rather than against the Fe assay of a single liquor stream.

Nickel, laterite, and other acidic sulfate systems

Iron and sulfur management is also relevant to nickel recovery from sulfide and lateritic materials. Low-temperature transformation of jarosite/goethite-derived iron phases, and laterite-nickel jarosite residues subjected to reduction roasting, illustrate how the selected iron-removal route constrains later residue treatment (Thibault et al., 2020; Zulhan et al., 2023). Although the jarosite process is not universally preferred in nickel circuits, these examples demonstrate that phase selection has downstream consequences for sulfur removal, reducibility, and metal recovery.

Secondary resources and recycling

Selective jarosite precipitation has been applied or investigated for leach solutions generated from secondary materials, including aerospace magnetic-material scraps and zinc-bearing wastes (Hazaveh et al., 2020; X. Zhou et al., 2024). Secondary-resource liquors can contain unusual impurity suites and higher concentrations of critical metals than primary-ore circuits. Their treatment, therefore, strengthens the case for feed-specific selectivity criteria and for residue characterization that tracks the deportment of valuable elements.

Comparison with Goethite, Hematite, and Alternative Iron-Removal Routes

Process-selection basis

Jarosite, goethite, and hematite are not interchangeable iron-removal products. They differ in formation conditions, sulfate incorporation, solid iron content, neutralization demand, residue mass, filtration behavior, and compatibility with upstream and downstream operations. Foundational and recent reviews of iron-precipitation residues emphasize that route selection should be based on the whole circuit rather than on Fe removal in isolation (Abadías Llamas et al., 2020; Dutrizac & Jambor, 2000; Höber & Steinlechner, 2021). The retained evidence does not support a universal ranking because plant constraints, energy prices, acid balance, metal value, and residue management options differ substantially.

Jarosite strengths and constraints

Jarosite is attractive in settings where acidic sulfate conditions are already present and simultaneous removal of Fe and part of the sulfate inventory is beneficial. It is commonly operated at moderate temperatures and near atmospheric pressure, but it produces a relatively large mass of sulfate-bearing residue and may incorporate valuable or hazardous elements. Its crystallinity can support separation, yet solid quality remains sensitive to precipitation history. These features make jarosite especially attractive when moderate-temperature operation and sulfate management outweigh the cost of larger residue generation.

Goethite and hematite alternatives

Goethite routes can produce iron-rich solids under less acidic conditions but often require careful control of redox and neutralization. Hematite routes generally target a higher-Fe, lower-volume residue but require more severe temperature and, in many implementations, pressure conditions. Resource-efficiency studies of pyrometallurgical and hydrometallurgical residue-management options, together with zinc- and nickel-residue studies, illustrate the broader trade-off between energy intensity, residue mass, and downstream recoverability (Abadías Llamas et al., 2020; Rämä et al., 2023; Thibault et al., 2020; Xing et al., 2024). A route that appears superior on residue mass alone may be less favorable when energy, equipment complexity, corrosion, or losses of valuable metals are included.

Table 7 is inserted here to convert the route comparison from a purely qualitative matrix to representative numerical operating ranges where defensible. These ranges are deliberately broad and should not be treated as design specifications.

Table 7. Representative operating ranges and process trade-offs for jarosite, goethite/paragoethite, and hematite iron-removal routes

Criterion	Jarosite	Goethite / paragoethite	Hematite	Interpretation
Typical temperature	≈80–100 °C for conventional JPP; lower-T routes also reported	Often ≈70–100 °C	Typically ≈180–230 °C in pressure systems	Representative ranges, not universal limits
Pressure	Usually atmospheric	Usually atmospheric	Frequently pressure-assisted	Equipment severity differs materially
Acidity / pH window	Acidic sulfate; many studies around pH ≈1–2 with controlled endpoint	Less acidic / stronger neutralization; redox-sensitive	High-T hydrolysis; route-specific acid balance	pH values are not directly comparable in concentrated liquors
Fe grade in solid	Often lower because sulfate/A-site species remain; continuous jarosite example 29.2–34.0 wt% Fe	Intermediate / process-dependent	Generally higher Fe fraction	Residue mass per Fe removed tends to decrease as Fe grade rises
Sulfate behavior	Structurally incorporated	Limited relative to jarosite	Limited relative to jarosite	Jarosite couples Fe removal with sulfate incorporation
Valuable-metal risk	Substitution, adsorption, occlusion and pore liquor	Co-precipitation/adsorption remain possible	Route-specific; high-T partitioning	No route is intrinsically selective without mass balance
Solid–liquid separation	Can be favorable with engineered crystals; quantitative filtration data sparse	Variable; process-specific	Often favorable crystalline product	Direct head-to-head filtration datasets are scarce
Best-fit logic	Moderate-severity acidic sulfate circuits needing controlled sulfate/Fe removal	Circuits favoring oxyhydroxide precipitation	When higher severity is justified by smaller/higher-Fe residue	Selection must be circuit-specific rather than ranked universally

Note. Representative ranges are synthesized from Dutrizac and Jambor (2000), Höber and Steinlechner (2021), Kaksonen et al. (2014a,b), and the comparative evidence discussed in this review. They are not universal design limits.

The table reinforces that the preferred route depends on the plant boundary. A high-iron hematite residue may reduce disposal mass, whereas jarosite may better fit an acidic sulfate circuit operating at moderate severity; neither advantage is universal.

Decision logic

A defensible route-selection exercise should evaluate at least six criteria: iron-removal efficiency, valuable-metal selectivity, reagent and energy intensity, solid–liquid separation, operational robustness, and residue outcome. These criteria should be weighted according to the circuit rather than collapsed into an unvalidated universal score. The process-selection framework proposed later in this review therefore treats jarosite, goethite, hematite, and other routes as alternatives whose suitability must be tested against a defined feed-and-downstream boundary.

Environmental Stability of Jarosite Precipitates

Stability is conditional, not intrinsic

Jarosite can be persistent under some acidic oxidizing conditions, but its long-term behavior changes with pH, redox potential, Fe(II) availability, organic ligands, microbial activity, substitution, and the identity of retained impurities. Laboratory and field-oriented studies document transformation to iron oxyhydroxides, reductive dissolution, changes in oxyanion mobility, and altered stability of substituted jarosites (Burton et al., 2021; Chen et al., 2021; Gao et al., 2020; Gao et al., 2021; González et al., 2020; Grigg, Wisawapipat, et al., 2024; Jin et al., 2024; Jin et al., 2023; Jin et al., 2020; Kölbl et al., 2021; Lee et al., 2025; Ryu & Kim, 2022; Tang et al., 2020; Yang et al., 2020; Zhang et al., 2025). The label “stable residue” is therefore incomplete unless the relevant disposal or reuse environment is specified.

Acidic, neutral, and reducing conditions

Under acidic conditions, dissolution rate depends on temperature, composition, and complexing ligands (Buriti et al., 2025a; Calla-Choque & Lapidus, 2021; Islas et al., 2020; Trueman et al., 2020). Near-neutral conditions can promote transformation rather than simple congruent dissolution, while reducing environments can destabilize ferric-iron frameworks and mobilize associated As, Sb, Pb, or other species (Chen et al., 2021; Gao et al., 2021; González et al., 2020; Jin et al., 2024; Jin et al., 2023; Lee et al., 2025; Yang et al., 2020). These pathways are especially relevant to saturated storage, organic-rich soils, remediation systems, and biological treatment.

Leaching toxicity and environmental interpretation

Bulk concentration alone is a poor predictor of environmental behavior. Leaching tests and mineralogical studies of jarosite residues, lead-bearing jarosites, and hydrometallurgical residues show that release depends on pH, test duration, liquid-to-solid ratio, phase assemblage, and transformation history (Huang et al., 2024; Peng, He, et al., 2023; Peng, Liu, et al., 2023; Ryu & Kim, 2022; R. Wang et al., 2020). Standardized testing is useful for comparison, but a single short-duration test should not be presented as proof of long-term stability.

Beneficial immobilization versus future liability

Jarosite's ability to bind hazardous oxyanions can be deliberately useful. Potassium-jarosite seeding has been investigated as a means of decreasing Pb and Asbioaccessibility, and modified jarosite has been used as an adsorbent for Cr(VI) and other contaminants (Picazo-Rodríguez et al., 2022; Sowers et al., 2023). The critical requirement is to distinguish temporary immobilization from durable stabilization. If subsequent reduction, hydrolysis, or recrystallization releases the bound element, an apparently beneficial capture step may simply defer the risk.

Treatment, Recycling, and Valorization of Jarosite Residues

Hydrometallurgical recovery of valuable metals

Jarosite residues are increasingly treated as secondary resources rather than terminal waste. Acid, alkaline, complexing-agent, and selective leaching routes have been reported for Ag, In, Zn, Pb, Cu, Cd, and other metals. Thiourea/oxalate systems, cyanide and non-cyanide leaching, alkaline decomposition, ionic liquids, and combined bioleaching–acid leaching illustrate the diversity of chemical approaches (Calla-Choque & Lapidus, 2020; Calla-Choque & Lapidus, 2021; Dávila-Pulido et al., 2025; De-la-Cruz-Moreno et al., 2021; Flores et al., 2022; Islas et al., 2021; Kushwaha & Agarwal, 2024; Nolasco et al., 2025; Picazo-Rodríguez et al., 2023; Singh et al., 2025). Their technical merit depends not only on extraction percentage but also on reagent recycle, impurity dissolution, solution purification, residue stability, and whether the recovered metal is actually upgraded to a saleable product.

Thermal decomposition, reduction, and pyrometallurgical routes

Thermal processing can decompose jarosite, remove sulfur, transform iron phases, and concentrate or recover valuable metals. Reported routes include cement-kiln treatment, CaO/SiO_2/CaSi-assisted pyrometallurgy, reduction roasting with biochar or other reductants, self-reducing briquettes, hydrothermal/thermal pre-treatment before hydrometallurgy, and recovery of Pb–Ag-bearing products (Ge et al., 2023; Ge

et al., 2024; Ge et al., 2025; Jiménez-Lugos, Flores-Favela, Romero-Serrano, Hernández-Ramírez, López-Rodríguez, Cruz-Ramírez, et al., 2024; Jiménez-Lugos, Flores-Favela, Romero-Serrano, Hernández-Ramírez, López-Rodríguez, Cuéllar-Herrera, et al., 2024; Kamberović et al., 2023; Lu et al., 2023; Mombelli et al., 2021; Olcay et al., 2025; Sanchez Vite et al., 2025; Xu et al., 2021; Zeng et al., 2023; S. Zhou et al., 2024; Zulhan et al., 2023). The principal trade-off is that thermal routes may improve phase separability and destroy unstable sulfate phases while increasing energy demand and transferring sulfur or volatile elements to off-gas treatment.

Chlorination, volatilization, and electrochemical processing

Selective chlorination and chloride volatilization have been proposed to extract or separate valuable metals from iron-rich precipitation residues, while slurry or suspension electrolysis offers an alternative route to combine iron recovery with detoxification (Höber et al., 2022; Qin & Haarberg, 2022; Steinlechner & Höber, 2022; Steinlechner & Witt, 2023; H. B. Wang et al., 2020; Wang et al., 2025). These processes are attractive when selective volatility or electrochemical potential differences can be exploited, but they require explicit accounting for chlorine-bearing reagents, off-gas or electrolyte management, corrosion, energy use, and secondary residues.

Biological and reductive treatment

Microbial systems can promote reductive dissolution, mineral transformation, or metal mobilization. Sulfate-reducing bacteria, Acidiphilium, Acidithiobacillus, iron-reducing bacteria, and biologically assisted recovery have all been examined (Chen et al., 2022; Fang et al., 2025; Gao et al., 2020; Gao et al., 2021; González et al., 2020; Lee et al., 2025; Ortiz-Castillo et al., 2021; Singh et al., 2023; Singh et al., 2025; Yang et al., 2020; Zhang et al., 2025). Biological routes may operate under mild thermal conditions, but the kinetics, control of redox conditions, nutrient requirements, and management of mobilized toxic elements remain important barriers to scale-up.

Materials applications

Jarosite-derived solids have been investigated as concrete constituents, adsorbents, calcium-sulfate products, magnetic or iron-bearing materials, and precursors for electrochemical materials. Examples include concrete valorization, Cr(VI) adsorption, calcium sulfate hemihydrate whiskers, reduced iron products, pyrrhotite-based sorbents, $FePO_4$/reduced-graphene-oxide cathode material, and direct utilization pathways for industrial jarosite (Ahamed et al., 2021; Cruz-Hernández et al., 2025; Ge et al., 2025; Pandiyan &Solaiyan, 2024; Picazo-Rodríguez et al., 2022; Tan et al., 2021; Xu et al., 2021; Xu et al., 2025; S. Zhou et al., 2024). These studies expand circularity options, but product performance must be evaluated together with contaminant stability, market size, quality consistency, and the mass fraction of the original residue that can realistically enter the application.

Integrated recovery and near-zero-waste concepts

Integrated flowsheets combine multiple operations to recover metals while transforming the iron-rich remainder into a less hazardous or more useful product. Examples include comprehensive recycling of zinc-hydrometallurgical residues, staged Pb–Ag/In recovery, hydrothermal phase transformation, and new separation processes for valuable metals (Chen et al., 2025; Conić et al., 2024; Janošević et al., 2023; Kamberović et al., 2021; Rämä et al., 2023; Y. Wang et al., 2020; Zeng et al., 2023; Zhou et al., 2025). The recurring weakness is system-boundary truncation: laboratory demonstrations often report metal extraction without closing water, reagent, energy, off-gas, and secondary-residue balances. Near-zero-waste claims should therefore be reserved for flowsheets that demonstrate where all major elements and process inputs leave the system.

Table 8 ranks representative valorization routes by evidence maturity rather than listing route types alone. Scale, feed realism, quantitative recovery, mass closure, and secondary-residue handling are treated as separate transferability criteria.

Table 8. Maturity matrix for jarosite-residue treatment and valorization routes

Route/example	Feed basis	Demonstrated scale	Quantitative outcome	Mass/secondary-residue closure	Transferability judgment
Hydrometallurgical selective leaching (Calla-Choque & Zárate-Silva, 2026)	Industrial jarosite	Laboratory	In recovery up to ≈98%; low Fe dissolution in reported condition	Partial	Promising selectivity; needs integrated reagent/water recycle and product purification
Kinetics-controlled Pb extraction (Yu et al., 2026)	Real Pb-bearing jarosite	Laboratory	Pb/Fe selectivity 14.74; Pb extraction 74.6%	Partial	Mechanistically strong; pilot energy/quench integration still needed
Reduction roasting + magnetic separation + backfill (Zhao et al., 2026b)	Real jarosite residue	Laboratory/engineering demonstration	Fe/Pb/Zn recovery and backfill route reported; iron concentrate and backfill quality quantified	Broader than most studies but plant closure not complete	Integrated flowsheet is stronger than single-step proof-of-concept; pilot campaign needed
Reduction roasting + in-situ sulfidation (Zhao et al., 2026a)	Real jarosite residue	Laboratory / response-surface optimization	Fe/Pb/Zn recovery optimized; engineering potential discussed	Partial	Promising integrated recovery; continuous validation and emissions accounting needed
Thermal/pyrometallurgical recovery (Ge et al.; Jiménez-Lugos et al.; Zhou et al.)	Real jarosite residues	Mostly laboratory/bench	Metal recovery and Fe-phase conversion are commonly reported	Often incomplete for gas/water/secondary solids	Technology maturity varies; product quality and off-gas closure are decisive
Materials/adsorbent/construction routes	Jarosite or treated residue	Laboratory/bench; some application-oriented tests	Mechanical/adsorption performance often reported	Market and contaminant-transfer closure commonly incomplete	A technically usable material is not automatically a circular outlet

Note. Author's synthesis based on the hydrometallurgical, thermal, biological, electrochemical, materials, and integrated-flowsheet studies cited in Section 11.

The table separates chemical feasibility from industrial maturity. This distinction is essential because many proposed valorization routes demonstrate extraction or product formation without closing the overall process balance.

Modeling, Scale-Up, Process Control, and Research Agenda

Thermodynamic and kinetic integration

Future models should couple ferric-sulfate speciation with non-ideal electrolyte behavior, phase competition, nucleation, growth, aggregation, and impurity incorporation. Existing precipitation, dissolution, and transformation studies provide the mechanistic pieces but rarely integrate them in a single predictive framework (Buriti et al., 2024; Buriti et al., 2025b; Cruells & Roca, 2022; Islas et al., 2020; Kamberović et al., 2023; Peng et al., 2024). The most important modeling advance would be to predict not only residual Fe but also which solid forms, its composition, and the evolution of its particle-size distribution.

Population balance and particle engineering

Particle-size distribution is a state variable that directly affects thickening and filtration. Population-balance approaches could connect nucleation rate, crystal growth, agglomeration, breakage, and solids recycle to measurable product-size distributions. Such models should be calibrated against particle-size data obtained with controlled dispersion protocols and validated against filtration or settling responses. Without this link, particle models remain disconnected from the process objective that matters to plant throughput.

Reactor hydrodynamics and scale-up

Scale-up requires more than preserving residence time. Mixing intensity, reagent injection location, local pH excursions, heat transfer, solids suspension, wall nucleation, and circulation patterns can change with vessel size. A practical research program should combine tracer-based residence-time distribution, computational fluid dynamics, local chemical measurements, and solids population tracking. The aim is not to build an unnecessarily complex model, but to identify which spatial gradients materially affect nucleation, impurity capture, and aggregate strength.

Process analytical technology and control

Jarosite precipitation is a strong candidate for state-based control because the important process state is not fully represented by pH alone. Useful measurements could include oxidation–reduction potential, temperature, free acidity by rapid titration, Fe(II)/Fe(III), sulfate, density, turbidity, particle-size proxies, and on-line elemental analysis where practical. Soft sensors could combine these measurements with reagent-addition and residence-time data to estimate supersaturation, solids inventory, and the risk of off-specification precipitation.

Industrial evidence gaps

The highest-priority gap is comparable industrial data. Future campaigns should report feed and discharge analyses on the same basis; complete Fe, sulfate, A-site-ion, and valuable-metal balances; reagent and energy consumption; washed and unwashed solid assays; particle-size distribution; filtration metrics; and uncertainty. Long-duration campaigns are especially important because impurity accumulation in recycled seeds, scaling, filter-cloth behavior, and gradual changes in liquor inventory cannot be reproduced in short laboratory tests.

Techno-economics, life cycle, and circularity

Resource-efficiency and residue-recovery studies show that the preferred iron-removal route can change when the system boundary expands beyond the precipitation reactor (Abadías Llamas et al., 2020; Höber & Steinlechner, 2021; Singh et al., 2023). Future techno-economic and life-cycle analyses should therefore compare reagent production, energy, water, residue transport, treatment, metal losses, avoided disposal, and recovered-product credits on a consistent functional basis. Circularity should not be claimed from the existence of a potential application alone; it requires a credible material outlet at the relevant scale and quality.

Proposed multi-criteria process-selection framework

This review proposes a six-gate decision logic with measurable indicators rather than an unqualified qualitative sequence. Gate 1 defines feed chemistry: Fe(II)/Fe(III), sulfate, free acidity, ionic strength, and valuable/hazardous-element inventory. Gate 2 selects the A-site species/reagent and neutralization strategy and records reagent/secondary-ion burdens. Gate 3 defines the reactor window using temperature, residence time, mixing/solids recycle, free acidity/pH, and residual Fe. Gate 4 verifies solid quality using PSD, settling, filtration resistance or flux, cake moisture, and washing efficiency. Gate 5 reconciles selectivity using valuable-metal loss, hazardous-element removal, washed/unwashed assays, and mass balance. Gate 6 assesses residue leachability/stability, recovery yield, energy/reagent envelope, secondary wastes, and—where available—TEA/LCA. Each gate should be classified as GO, CONDITIONAL GO, or STOP/REROUTE using plant-specific acceptance limits. The review deliberately avoids inventing universal numerical thresholds.

Figure 6 is inserted here as the operational synthesis of the review. Each gate now lists measurable evidence and explicit GO / CONDITIONAL GO / STOP–REROUTE outcomes while leaving numerical acceptance limits to plant-specific calibration.

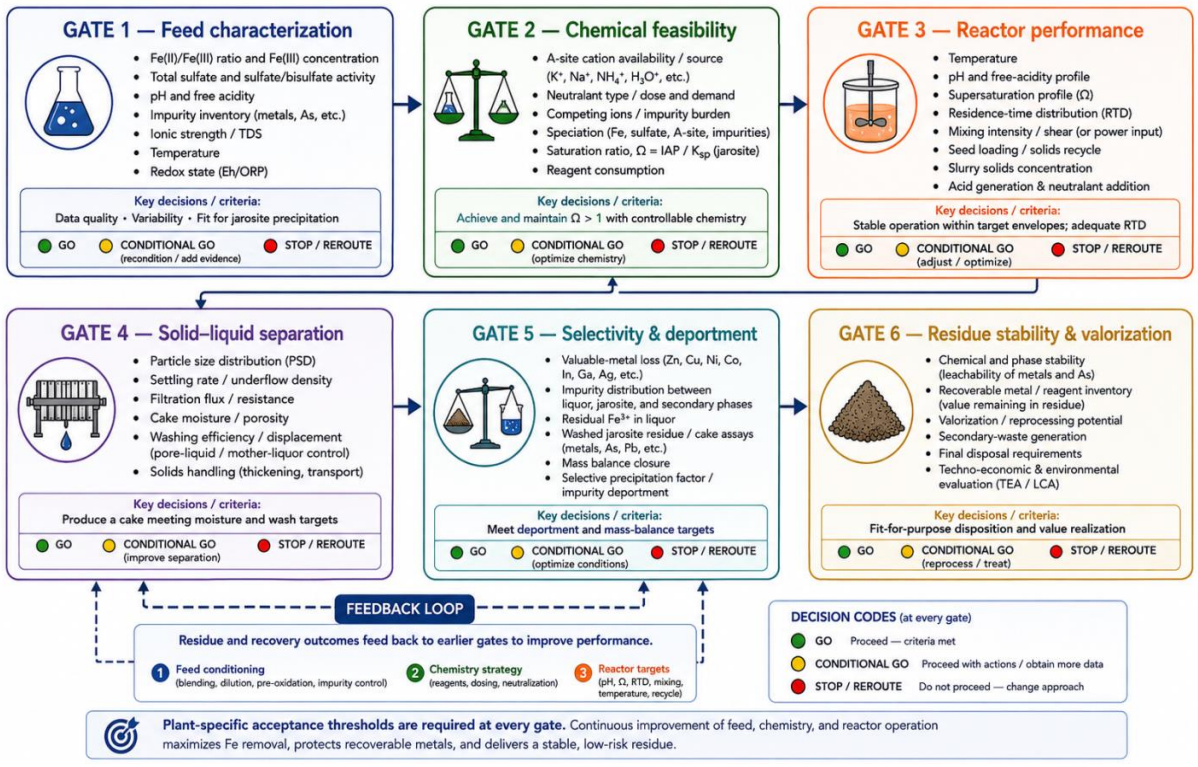

Figure 6. Integrated multi-criteria process-selection framework for jarosite precipitation

Note. Author's conceptual synthesis based on the critical review. The framework is qualitative and requires plant-specific validation before use as an operating rule.

The feedback loop is intentional: residue behavior and downstream recovery performance should update precipitation targets, A-site species/reagent choice, and feed-conditioning strategy rather than being treated as end-of-pipe consequences.

Research priorities

The most consequential research priorities are high-ionic-strength activity/speciation models, time-resolved nucleation/growth measurements, population balances linked to measured PSD, standardized impurity-deportment mass balances, direct filtration/washing measurements, continuous pilot campaigns, long-term residue-transformation tests, and integrated TEA/LCA. The revised tables make the evidence deficit visible: several studies quantify Fe removal or kinetics, but directly comparable filtration resistance, cake moisture, wash efficiency, and complete mass closure remain uncommon. Future campaigns should report the full reaction–particle–separation–residue chain on one reconciled basis.

Conclusions

Jarosite remains a technically relevant iron-precipitation route for acidic sulfate hydrometallurgy, but its performance cannot be judged by ferric-iron removal alone. The revised quantitative synthesis shows that operating conditions, kinetic parameters, impurity losses, and particle properties are strongly system-dependent; therefore, universal optimum values are not defensible without matching the solution chemistry and process boundary. Selectivity must be demonstrated by reconciled valuable-metal and hazardous-element balances, not inferred from a low residual Fe concentration. Solid quality is a primary process response because particle-size distribution, aggregate strength, settling, filtration resistance, cake moisture, and washing determine whether a chemically successful precipitation step can operate reliably at scale. Residue stability is contingent on exposure chemistry and transformation history, while valorization routes vary widely in maturity and often lack complete closure of reagents, water, energy, off-gas, and secondary residues. The proposed six-gate framework converts these findings into measurable plant decisions while deliberately avoiding universal cut-offs. The most important evidence needs include high-ionic-strength process-chemistry models, comparable kinetic reporting, direct solid–liquid-separation data, continuous campaigns, closed mass balances, and integrated techno-economic and life-cycle assessment. These additions differentiate the present review from broader prior jarosite reviews by making industrial transferability and quantitative decision evidence the central analytical objective.

Declarations

Funding: No external funding was received for the preparation of this review.

Conflicts of interest: The author declares no known competing financial interests or personal relationships that could have influenced the work reported in this manuscript.

Data availability: No new experimental data were generated. The review is based on the cited literature and the revised bibliographic audit updated through 8 August 2026. Quantitative values reported in synthesis tables retain the basis stated in the original sources.

Author contributions: Antonio Clareti Pereira: Conceptualization, methodology, investigation, critical analysis, visualization, writing—original draft, and writing—review and editing.

References

1. Abadías Llamas, A., Bartie, N. J., Heibeck, M., Stelter, M., & Reuter, M. A. (2020). Resource efficiency evaluation of pyrometallurgical solutions to minimize iron-rich residues in the roast-leach-electrowinning process. In A. Siegmund, S. Alam, J. Grogan, U. Kerney, & E. Shibata (Eds.), *PbZn 2020: 9th International Symposium on Lead and Zinc Processing* (pp. 351–364). Springer. https://doi.org/10.1007/978-3-030-37070-1_31
2. Ahamed, A. M., Pons, M.-N., Ricoux, Q., Issa, S., Goettmann, F., &Lapicque, F. (2021). New pathway for utilization of jarosite, an industrial waste of zinc hydrometallurgy. *Minerals Engineering, 170*, Article 107030. https://doi.org/10.1016/j.mineng.2021.107030
3. Aromataris, E., & Munn, Z. (Eds.). (2020). *JBI manual for evidence synthesis*. JBI. https://doi.org/10.46658/JBIMES-20-01
4. Asimi Neisiani, A., Moosakazemi, F., &Chehreh Chelgani, S. (2023). Technical and economic comparison between sodium and ammonium agents in the jarosite precipitation process—An evaluation for industrial applications. *ACS Omega, 8*(39), 36001–36007. https://doi.org/10.1021/acsomega.3c03536
5. Asimi, A., Gharibi, K., Abkhoshk, E., Moosakazemi, F., & Chehreh Chelgani, S. (2020). Effects of operational parameters on the low contaminant jarosite precipitation process—An industrial scale study. *Materials, 13*(20), Article 4662. https://doi.org/10.3390/ma13204662
6. Buriti, M. D. S., Cézac, P., & Casás, L. (2024). Dissolution and precipitation of jarosite-type compounds: State of the art and future perspectives. *Comptes Rendus. Chimie, 27*(S4), 81–109. https://doi.org/10.5802/crchim.321
7. Buriti, M. D. S., Poulain, M., Cézac, P., & Casás, L. (2025a). Assessing jarosite kinetic dissolution rates at

acidic conditions and different temperatures. *Minerals, 15*(9), Article 965. https://doi.org/10.3390/min15090965

8. Buriti, M. D. S., Poulain, M., Cézac, P., & Casás, L. (2025b). K-jarosite precipitation kinetics at low-moderate temperatures: Factors affecting mechanism, formation rates, solid morphology and crystallinity. *Hydrometallurgy, 235*, Article 106474. https://doi.org/10.1016/j.hydromet.2025.106474
9. Burton, E. D., Karimian, N., Johnston, S. G., Schoepfer, V. A., Choppala, G., & Lamb, D. (2021). Arsenic-imposed effects on schwertmannite and jarosite formation in acid mine drainage and coupled impacts on arsenic mobility. *ACS Earth and Space Chemistry, 5*(6), 1418–1435. https://doi.org/10.1021/acsearthspacechem.1c00047
10. Calla-Choque, D., & Lapidus, G. T. (2020). Acid decomposition and silver leaching with thiourea and oxalate from an industrial jarosite sample. *Hydrometallurgy, 192*, Article 105289. https://doi.org/10.1016/j.hydromet.2020.105289
11. Calla-Choque, D., & Lapidus, G. T. (2021). Jarosite dissolution kinetics in the presence of acidic thiourea and oxalate media. *Hydrometallurgy, 200*, Article 105565. https://doi.org/10.1016/j.hydromet.2021.105565
12. Calla-Choque, D., & Zárate-Silva, L. E. (2026). Effect of phosphate on indium recovery with pyrophosphate from industrial jarosite in alkaline medium. *MRS Advances, 11*, 359–364. https://doi.org/10.1557/s43580-026-01620-9
13. Chen, H.-R., Zhang, D.-R., Nie, Z.-Y., Xia, J.-L., Li, Q., Zhang, R.-Y., Yin, H.-H., & Pakostova, E. (2022). Reductive dissolution of jarosite by inorganic sulfur compounds catalyzed by *Acidithiobacillus thiooxidans*. *Hydrometallurgy, 212*, Article 105908. https://doi.org/10.1016/j.hydromet.2022.105908
14. Chen, K., Jin, X., Guo, C., He, C., Zhang, Y., Gao, K., Lu, G., & Dang, Z. (2021). Reductive dissolution of Pb–Zn jarosite under near-neutral conditions. *Chemical Geology, 579*, Article 120338. https://doi.org/10.1016/j.chemgeo.2021.120338.
15. Chen, M., Wang, R., Fan, W., Wang, J., Zeng, X., Han, Y., Liang, Q., Huang, R., Zhou, S., & Shu, J. (2025). Advances on jarosite residue detoxification and reutilization: A review. *Environmental Science and Pollution Research, 32*(7), 3571–3592. https://doi.org/10.1007/s11356-025-35907-5
16. Conić, V., Janošević, M., Božić, D. S., Avramović, L., Jovanović, I., Bugarin, D. M., & Đorđievski, S. (2024). Copper, zinc, and lead recovery from jarosite Pb–Ag tailings waste (Part 2). *Minerals, 14*(8), Article 791. https://doi.org/10.3390/min14080791
17. Cruells, M., & Roca, A. (2022). Jarosites: Formation, structure, reactivity and environmental. *Metals, 12*(5), Article 802. https://doi.org/10.3390/met12050802
18. Cruz-Hernández, M., García-Cerón, A., Salinas Maldonado, R. G., Corro-Escorcia, I. A., Hernández-Ávila, J., Cerecedo-Sáenz, E., Flores-Badillo, J., Toro, N., Saldaña, M., Gutiérrez-Amador, M. P., Barrientos-Hernández, F. R., & Salinas-Rodríguez, E. (2025). Leveraging industrial jarosite waste for arsenic (V) and chromium(III) adsorption from water: A preliminary study. *Applied Sciences, 15*(3), Article 1469. https://doi.org/10.3390/app15031469
19. Dávila-Pulido, G. I., González-Bonilla, B. R., Charles, D. A., González-Ibarra, A. A., Cháidez-Félix, J. C., & Salinas-Rodríguez, A. (2025). Silver extraction from jarositic waste: Effect of sodium silicate on cyanidation and alkaline decomposition as a path to revalorization. *Journal of Sustainable Metallurgy, 11*(3), 2622–2631. https://doi.org/10.1007/s40831-025-01161-9
20. De-la-Cruz-Moreno, J. E., Ceniceros-Gómez, A. E., Morton-Bermea, O., & Hernández-Álvarez, E. (2021). Recovery of indium from jarosite residues of zinc refinery by a hydrometallurgical process. *Hydrometallurgy, 203*, Article 105697. https://doi.org/10.1016/j.hydromet.2021.105697
21. Dong, W., Qiu, X., Zhao, W., Guo, B., & Jiang, K. (2025). The evolution of Ga/In occurrence state and their dependence on jarosite during the precipitation enrichment for recovery of scattering metals and Cu from Zn leaching solution. *Sustainable Materials and Technologies, 45*, Article e01446. https://doi.org/10.1016/j.susmat.2025.e01446
22. Dutrizac, J. E., &Jambor, J. L. (2000). Jarosites and their application in hydrometallurgy. *Reviews in Mineralogy and Geochemistry, 40*(1), 405–452. https://doi.org/10.2138/rmg.2000.40.8
23. Fang, J., Yang, H., Song, Y., Sun, Q., & Lin, D. (2025). Feasibility analysis of sulfate-reducing bacteria-loaded coke on the reduction and mineralization of jarosite residues. *Process Safety and Environmental Protection, 194*, 1159–1171. https://doi.org/10.1016/j.psep.2024.12.087
24. Flores, V. H., Patiño, F., Roca, A., Flores, M. U., Reyes, I. A., Reyes, M., & Islas, H. (2022). Alkaline decomposition of solid solution of ammonium–sodium jarosite with arsenic. *Metals, 12*(4), Article 584. https://doi.org/10.3390/met12040584
25. Gao, K., Hu, Y., Guo, C., Ke, C., He, C., Hao, X., Lu, G., & Dang, Z. (2020). Effects of adsorbed phosphate on jarosite reduction by a sulfate-reducing bacterium and associated mineralogical transformation. *Ecotoxicology and Environmental Safety, 202*, Article 110921. https://doi.org/10.1016/j.ecoenv.2020.110921
26. Gao, K., Hu, Y., Guo, C., Ke, C., Lu, G., & Dang, Z. (2021). Mobilization of arsenic during reductive dissolution of As (V)-bearing jarosite by a sulfate-reducing bacterium. *Journal of Hazardous Materials,*

402, Article 123717. https://doi.org/10.1016/j.jhazmat.2020.123717

27. Ge, H., Pan, Z., Xie, F., Lu, D., Wang, W., & Wu, S. (2023). Recovery of valuable metals by roasting of jarosite in cement kiln. *Metals*, *13*(2), Article 250. https://doi.org/10.3390/met13020250
28. Ge, H., Xie, F., Wu, S., & Wang, W. (2024). Cleaner recycling of jarosite residue by $Ca(OH)_2$ leaching–biomass magnetization roasting. *JOM*, *76*(11), 6639–6649. https://doi.org/10.1007/s11837-024-06825-7
29. Ge, H., Xie, F., Wu, S., Wang, W., Chen, P., & Wang, Z. (2025). Preparation of reduced iron powder by reduction roasting of jarosite residue using straw-type biochar reductant. *Biomass and Bioenergy*, *193*, Article 107539. https://doi.org/10.1016/j.biombioe.2024.107539
30. González, E., Hernández, L., Muñoz, J. Á., Blázquez, M. L., Ballester, A., & González, F. (2020). Electron shuttles stimulate the reductive dissolution of jarosite by *Acidiphiliumcryptum*. *Hydrometallurgy*, *194*, Article 105351. https://doi.org/10.1016/j.hydromet.2020.105351
31. Grigg, A. R. C., Notini, L., Kaegi, R., Thomas Arrigo, L. K., & Kretzschmar, R. (2024). Aluminium substitution affects jarosite transformation to iron oxyhydroxides in the presence of aqueous Fe (II). *Geochimica et Cosmochimica Acta*, *374*, 72–84. https://doi.org/10.1016/j.gca.2024.04.008
32. Grigg, A. R. C., Wisawapipat, W., Barmettler, K., Schulz, K., Notini, L., Thomas Arrigo, L. K., & Kretzschmar, R. (2024). Stability and transformation of jarosite and Al-substituted jarosite in an acid sulfate paddy soil under laboratory and field conditions. *Geochimica et Cosmochimica Acta*, *382*, 128–141. https://doi.org/10.1016/j.gca.2024.07.026
33. Khanmohammadi Hazaveh, P., Karimi, S., Rashchi, F., & Sheibani, S. (2020). Purification of the leaching solution of recycling zinc from the hazardous electric arc furnace dust through an As-bearing jarosite. *Ecotoxicology and Environmental Safety*, *202*, Article 110893. https://doi.org/10.1016/j.ecoenv.2020.110893
34. Höber, L., & Steinlechner, S. (2021). A comprehensive review of processing strategies for iron precipitation residues from zinc hydrometallurgy. *Cleaner Engineering and Technology*, *4*, Article 100214. https://doi.org/10.1016/j.clet.2021.100214
35. Höber, L., Witt, K., & Steinlechner, S. (2022). Selective chlorination and extraction of valuable metals from iron precipitation residues. *Applied Sciences*, *12*(7), Article 3590. https://doi.org/10.3390/app12073590
36. Hu, J., Wang, Q., Xiao, Z., Wang, Z., Zeng, J., Liu, W., Lin, Z., Qi, C., & Li, X. (2025). Pb substitution in natrojarosite: Microstructural changes and effects on As(V) and Cr(VI) adsorption. *Colloids and Surfaces A: Physicochemical and Engineering Aspects*, *723*, Article 137363. https://doi.org/10.1016/j.colsurfa.2025.137363
37. Huang, Y., Zhou, C., Quan, Y., Xu, S., Li, Q., & Liu, G. (2024). Elements characteristics and potential environmental risk assessment of jarosite residue and arsenic sulfide residue based on geochemical and mineralogical analysis. *Science of the Total Environment*, *944*, Article 173600. https://doi.org/10.1016/j.scitotenv.2024.173600
38. Islas, H., Flores, M. U., Juárez, J. C., Reyes, M., Blanco, A., Gutiérrez, E. J., Aguilar, J., Nolasco, M. C., Rodríguez, I., & Reyes, I. A. (2021). Silver leaching from jarosite-type compounds using cyanide and non-cyanide lixiviants: A kinetic approach. *Minerals Engineering*, *174*, Article 107250. https://doi.org/10.1016/j.mineng.2021.107250.
39. Islas, H., Flores, M. U., Reyes, I. A., Juárez, J. C., Reyes, M., Teja, A. M., Palacios, E. G., Pandiyan, T., & Aguilar-Carrillo, J. (2020). Determination of the dissolution rate of hazardous jarosites in different conditions using the shrinking core kinetic model. *Journal of Hazardous Materials*, *386*, Article 121664. https://doi.org/10.1016/j.jhazmat.2019.121664
40. Janošević, M., Conić, V., Božić, D., Avramović, L., Jovanović, I., Kamberović, Ž., & Marjanović, S. (2023). Indium recovery from jarosite Pb–Ag tailings waste (Part 1). *Minerals*, *13*(4), Article 540. https://doi.org/10.3390/min13040540
41. Jiménez-Lugos, C., Flores-Favela, M., Romero-Serrano, A., Hernández-Ramírez, A., López-Rodríguez, J., Cruz-Ramírez, A., & Colin-García, E. (2024). Pyrometallurgical treatment of jarosite residue with a mixture of CaO, SiO_2, and CaSi. *Journal of Mining and Metallurgy, Section B: Metallurgy*, *60*(2), 205–214. https://doi.org/10.2298/JMMB231219015J
42. Jiménez-Lugos, C., Flores-Favela, M., Romero-Serrano, A., Hernández-Ramírez, A., López-Rodríguez, J., Cuéllar-Herrera, L., & Colin-García, E. (2024). Recovery of silver and lead from jarosite residues by roasting and reducing pyrometallurgical processes. *Metals*, *14*(8), Article 954. https://doi.org/10.3390/met14080954
43. Jin, X., Guo, C., Huang, Q., Tao, X., Li, X., Xie, Y., Dang, Z., Zhou, J., & Lu, G. (2024). Arsenic redistribution associated with Fe(II)-induced jarosite transformation in the presence of polygalacturonic acid. *Science of the Total Environment*, *935*, Article 173444. https://doi.org/10.1016/j.scitotenv.2024.173444
44. Jin, X., Huang, Q., Li, X., Lu, G., Yao, Q., Xu, F., Guo, C., & Dang, Z. (2023). Divergent repartitioning of antimony and arsenic during jarosite transformation: A comparative study under aerobic and anaerobic conditions. *Science of the Total Environment*, *898*, Article 165533. https://doi.org/10.1016/j.scitotenv.2023.165533

45. Jin, X., Li, X., Guo, C., Jiang, M., Yao, Q., Lu, G., & Dang, Z. (2020). Fate of oxalic-acid-intervened arsenic during Fe(II)-induced transformation of As(V)-bearing jarosite. *Science of the Total Environment, 719*, Article 137311. https://doi.org/10.1016/j.scitotenv.2020.137311
46. Kaksonen, A. H., Morris, C., Rea, S., Li, J., Wylie, J., Usher, K. M., Ginige, M. P., Cheng, K. Y., Hilario, F., & du Plessis, C. A. (2014). Biohydrometallurgical iron oxidation and precipitation: Part I—Effect of pH on process performance. *Hydrometallurgy, 147–148*, 255–263. https://doi.org/10.1016/j.hydromet.2014.04.016
47. Kaksonen, A. H., Morris, C., Rea, S., Li, J., Usher, K. M., McDonald, R. G., Hilario, F., Hosken, T., Jackson, M., & du Plessis, C. A. (2014). Biohydrometallurgical iron oxidation and precipitation: Part II—Jarosite precipitate characterisation and acid recovery by conversion to hematite. *Hydrometallurgy, 147–148*, 264–272. https://doi.org/10.1016/j.hydromet.2014.04.015
48. Kamberović, Ž., Gajić, N., Korać, M., Jevtić, S., Sokić, M., & Stojanović, J. (2021). Technologically sustainable route for metals valorization from jarosite-PbAg sludge. *Minerals, 11*(3), Article 255. https://doi.org/10.3390/min11030255
49. Kamberović, Ž., Ranitović, M., Manojlović, V., Jevtić, S., Gajić, N., &Štulović, M. (2023). Thermodynamic and kinetic analysis of jarosite Pb–Ag sludge thermal decomposition for hydrometallurgical utilization of valuable elements. *Journal of Thermal Analysis and Calorimetry, 148*(21), 11799–11810. https://doi.org/10.1007/s10973-023-12508-3
50. Karimian, N., Johnston, S. G., Tavakkoli, E., Frierdich, A. J., & Burton, E. D. (2023). Mechanisms of arsenic and antimony co-sorption onto jarosite: An X-ray absorption spectroscopic study. *Environmental Science & Technology, 57*(12), 4813–4820. https://doi.org/10.1021/acs.est.2c08213
51. Kölbl, A., Kaiser, K., Winkler, P., Mosley, L., Fitzpatrick, R., Marschner, P., Wagner, F. E., Häusler, W., & Mikutta, R. (2021). Transformation of jarosite during simulated remediation of a sandy sulfuric soil. *Science of the Total Environment, 773*, Article 145546. https://doi.org/10.1016/j.scitotenv.2021.145546
52. Kushwaha, P., & Agarwal, M. (2024). Efficient extraction of metals (Fe, Zn, Pb) from hazardous jarosite using ionic liquid and waste-derived solvents. *Environmental Science and Pollution Research, 31*(27), 39533–39548. https://doi.org/10.1007/s11356-024-33811-y
53. Lee, M., Kim, Y., Roh, Y., & Kim, Y. (2025). Reductive transformation of oxyanion-containing jarosite by iron-reducing bacteria: Effects of mineral precipitation on the mobility of potentially toxic elements. *Journal of Hazardous Materials Advances, 19*, Article 100804. https://doi.org/10.1016/j.hazadv.2025.100804
54. Lu, D., Bai, Y., Wang, W., Fu, Y., Xie, F., Chang, Y., & Han, Y. (2023). Thermal decomposition process analysis of jarosite residue. *Metals, 13*(2), Article 261. https://doi.org/10.3390/met13020261
55. Mombelli, D., Gonçalves, D. L., Mapelli, C., Barella, S., & Gruttadauria, A. (2021). Processing and characterization of self-reducing briquettes made of jarosite and blast furnace sludges. *Journal of Sustainable Metallurgy, 7*(4), 1603–1626. https://doi.org/10.1007/s40831-021-00419-2
56. Nolasco, M. C., Rodríguez, I., Vilasó, J. E., Flores, M. U., Pandiyan, T., Gutiérrez, E. J., Aguilar, J., Reyes, M., & Reyes, I. A. (2025). Selective extraction of silver from jarosite residues produced in the zinc hydrometallurgical process using thiourea under acidic conditions: Kinetic analysis and leaching optimization. *Hydrometallurgy, 231*, Article 106396. https://doi.org/10.1016/j.hydromet.2024.106396
57. Oladipo, B., &Ojumu, T. V. (2023). Influence of solution pH on the properties of biogenic jarosite produced from ferrous ion bio-oxidation in a bioreactor. *Hydrometallurgy, 221*, Article 106144. https://doi.org/10.1016/j.hydromet.2023.106144
58. Olcay, R. H., Palacios, E. G., Reyes, I. A., Patiño, F., Reyes, M., Pérez, M., Islas, H., Juárez, J. C., & Flores, M. U. (2025). Behavior of toxic elements in the thermal decomposition of industrial sodium jarosite: A kinetic analysis. *Reaction Kinetics, Mechanisms and Catalysis, 138*(1), 107–124. https://doi.org/10.1007/s11144-024-02709-8.
59. Ortiz-Castillo, J. E., Mirazimi, M., Mohammadi, M., Dy, E., & Liu, W. (2021). The role of microorganisms in the formation, dissolution, and transformation of secondary minerals in mine rock and drainage: A review. *Minerals, 11*(12), Article 1349. https://doi.org/10.3390/min11121349
60. Page, M. J., McKenzie, J. E., Bossuyt, P. M., Boutron, I., Hoffmann, T. C., Mulrow, C. D., Shamseer, L., Tetzlaff, J. M., Akl, E. A., Brennan, S. E., Chou, R., Glanville, J., Grimshaw, J. M., Hróbjartsson, A., Lalu, M. M., Li, T., Loder, E. W., Mayo-Wilson, E., McDonald, S., . . . Moher, D. (2021). The PRISMA 2020 statement: An updated guideline for reporting systematic reviews. *BMJ, 372*, Article n71. https://doi.org/10.1136/bmj.n71
61. Pandiyan, T. K., & Solaiyan, E. (2024). Sustainable valorization of jarosite as a concrete material: Investigation of hydration, mechanical, and durability properties. *Journal of Sustainable Metallurgy, 10*(4), 2352–2375. https://doi.org/10.1007/s40831-024-00936-w
62. Peng, J., He, L., Liu, H., Sun, Z., & Yan, X. (2023). The synthesis of lead-bearing jarosite and its

occurrence characteristic and leaching toxicity evaluation. *Metals*, *13*(5), Article 941. https://doi.org/10.3390/met13050941

63. Peng, J., Liu, H., He, L., Sun, Z., Peng, Y., Huang, X., & Yan, X. (2023). Physicochemical properties and leaching toxicity assessment of jarosite residue. *Sustainability*, *15*(12), Article 9472. https://doi.org/10.3390/su15129472
64. Peng, X., Jin, X., Zhen, Y., Yang, B., Li, X., Wei, C., Deng, Z., Li, M., & Fan, G. (2024). Hydrothermal crystallization of jarosite and natrojarosite from acid leaching solution of zinc oxide dust. *Canadian Metallurgical Quarterly*, *63*(4), 1449–1462. https://doi.org/10.1080/00084433.2023.2257569
65. Pereira, A. C. (2026). Jarosite in mineral processing and hydrometallurgy: A structured critical review of formation, treatment, environmental risk, and circular valorization (2020–2025). *Journal International Review of Research Studies*, *1*(10), 1–58. https://doi.org/10.66104/1vvk3x48Picazo-Rodríguez, N. G., Carrillo-Pedroza, F. R., Soria-Aguilar, M. de J., Baltierra, G., González, G., Martínez-Luévanos, A., & Almaguer Guzmán, I. (2022). Use of thermally modified jarosite for the removal of hexavalent chromium by adsorption. Crystals, 12(1), 80.
66. Picazo-Rodríguez, N. G., Carrillo-Pedroza, F. R., Soria-Aguilar, M. de J., Baltierra, G., González, G., Martinez-Luevanos, A., & Almaguer Guzmán, I. (2022). Use of thermally modified jarosite for the removal of hexavalent chromium by adsorption. *Crystals*, *12*(1), Article 80. https://doi.org/10.3390/cryst12010080
67. Picazo-Rodríguez, N. G., Soria-Aguilar, M. de J., Chaidez, J., Flores, M., Almaguer-Guzmán, I., & Carrillo-Pedroza, F. R. (2023). Analysis of the behavior of As and Pb during the pretreatments applied to a jarosite residue for the recovery of gold and silver. *Metals*, *13*(1), Article 138. https://doi.org/10.3390/met13010138
68. Qin, B., & Haarberg, G. M. (2022). The study of jarosite waste used for suspension electrolysis in aqueous NaOH electrolyte. *Journal of The Electrochemical Society*, *169*(7), Article 073506. https://doi.org/10.1149/1945-7111/ac7dca
69. Qin, S.-C., Jiang, K.-X., Wang, H.-B., Zhang, B.-S., Wang, Y.-F., & Zhang, X.-D. (2020). Research on behavior of iron in the zinc sulfide pressure leaching process. *Minerals*, *10*(3), Article 224. https://doi.org/10.3390/min10030224
70. Rämä, M., Klemettinen, L., Rinne, M., Taskinen, P., Michallik, R. M., Salminen, J., & Jokilaakso, A. (2023). Processing of a zinc leach residue by a non-fossil reductant. *ACS Omega*, *8*(24), 21450–21463. https://doi.org/10.1021/acsomega.3c00250.
71. Ryu, J.-G., & Kim, Y. (2022). Mineral transformation and dissolution of jarosite coprecipitated with hazardous oxyanions and their mobility changes. *Journal of Hazardous Materials*, *427*, Article 128283. DOI: 10.1016/j.jhazmat.2022.128283. DOI 10.1016/j.jhazmat.2022.128283
72. Sánchez Vite, J. E., Cruz Ramírez, A., Flores Favela, M. E., Sánchez Alvarado, R. G., Romero Serrano, J. A., García Hernández, M., Jiménez Romero, T. del R., & Jiménez Lugos, J. C. (2025). Thermodynamic assessment of the pyrometallurgical recovery of a Pb–Ag alloy from a mixture of ammonium jarosite–lead paste wastes. *Recycling*, *10*(4), Article 136. DOI: 10.3390/recycling10040136. DOI 10.3390/recycling10040136
73. Shi, M., Min, X., Tian, C., Hao, T., Zhu, S., Ge, Y., Wang, Q., Yan, X., & Lin, Z. (2022). Mechanisms of Pb(II) coprecipitation with natrojarosite and its behavior during acid dissolution. *Journal of Environmental Sciences*, *122*, 128–137. DOI: 10.1016/j.jes.2021.10.006. DOI 10.1016/j.jes.2021.10.006
74. Shi, M., Min, X., Zhang, W., Li, K., Wu, J., Ai, Z., Ke, Y., Wang, Q., & Yan, X. (2023). (Na, Pb)-jarosite nucleation and growth on anglesite: Implications for inhibition of Pb releasing. *Science of the Total Environment*, *901*, Article 165972. DOI: 10.1016/j.scitotenv.2023.165972. DOI 10.1016/j.scitotenv.2023.165972
75. Singh, V. K., Manna, S., Biswas, J. K., & Pugazhendhi, A. (2023). Recovery of residual metals from jarosite waste using chemical and biochemical processes to achieve sustainability: A state-of-the-art review. *Journal of Environmental Management*, *343*, Article 118221. DOI: 10.1016/j.jenvman.2023.118221. DOI 10.1016/j.jenvman.2023.118221
76. Singh, V. K., Saxena, P., & Manna, S. (2025). Recovery of cadmium, lead, strontium and zinc from jarosite waste by using a combinatory approach of bioleaching and acid leaching. *Canadian Metallurgical Quarterly*, *64*(3), 1449–1457. DOI: 10.1080/00084433.2024.2393028. DOI 10.1080/00084433.2024.2393028
77. Sowers, T. D., Blackmon, M. D., Betts, A. R., Jerden, M. L., Scheckel, K. G., & Bradham, K. D. (2023). Potassium jarosite seeding of soils decreases lead and arsenic bioaccessibility: A path toward concomitant remediation. *Proceedings of the National Academy of Sciences of the United States of America*, *120*(50), Article e2311564120. DOI: 10.1073/pnas.2311564120. DOI 10.1073/pnas.2311564120
78. Steinlechner, S., & Höber, L. (2022). CO_2-optimized recovery of special metals from precipitation residue by selective chlorination. In T. Ouchi, G. Azimi, K. Forsberg, H. Kim, S. Alam, N. R. Neelameggham, A. A. Baba, & H. Peng (Eds.), *Rare Metal Technology*

2022 (pp. 237–244). Springer. DOI: 10.1007/978-3-030-92662-5_23. DOI 10.1007/978-3-030-92662-5_23

79. Steinlechner, S., & Witt, K. (2023). Simultaneous extraction of valuable metals from iron-containing residues by selective chlorination and evaporation. *Mining, Metallurgy & Exploration*, *40*(6), 2023–2036. DOI: 10.1007/s42461-023-00872-5. DOI 10.1007/s42461-023-00872-5
80. Sun, P., Wang, J., Li, X., Wei, C., Deng, Z., & Li, M. (2025). The behavior of zinc, copper, and indium during the precipitation of lead jarosite. *JOM*, *77*(1), 303–312. DOI: 10.1007/s11837-024-06989-2. DOI 10.1007/s11837-024-06989-22.
81. Tan, H., Ma, X., Dong, F., Li, Y., Wang, J., & Yang, F. (2021). Preparation of calcium sulfate hemihydrate whiskers from complex jarosite waste. *Materials and Technology*, *55*(3), 467–473. https://doi.org/10.17222/mit.2020.251DOI 10.17222/mit.2020.251
82. Tang, Y., Xie, Y., Lu, G., Ye, H., Dang, Z., Wen, Z., Tao, X., Xie, C., & Yi, X. (2020). Arsenic behavior during gallic acid-induced redox transformation of jarosite under acidic conditions. *Chemosphere*, *255*, Article 126938. https://doi.org/10.1016/j.chemosphere.2020.126938 DOI 10.1016/j.chemosphere.2020.126938
83. Thibault, Y., McEvoy, J. G., & Beauchemin, S. (2020). Iron and sulphur management options during Ni recovery from (bio) leaching of pyrrhotite tailings, Part 1: Mechanisms of low-temperature transformation from goethite and jarosite to magnetic spinel. *Minerals Engineering*, *150*, Article 106265. https://doi.org/10.1016/j.mineng.2020.106265 DOI 10.1016/j.mineng.2020.106265
84. Trueman, A. M., McLaughlin, M. J., Mosley, L. M., & Fitzpatrick, R. W. (2020). Composition and dissolution kinetics of jarosite-rich segregations extracted from an acid sulfate soil with sulfuric material. *Chemical Geology*, *543*, Article 119606. https://doi.org/10.1016/j.chemgeo.2020.119606 DOI 10.1016/j.chemgeo.2020.119606
85. Wang, H. B., Zheng, C. Z., & Qin, S. C. (2020). Study of a novel chloride volatilization process for the treatment of jarosite residue. In A. Siegmund, S. Alam, J. Grogan, U. Kerney, & E. Shibata (Eds.), *PbZn 2020: 9th International Symposium on Lead and Zinc Processing* (pp. 835–845). Springer. https://doi.org/10.1007/978-3-030-37070-1_73 DOI 10.1007/978-3-030-37070-1_73
86. Wang, R., Chen, M., Fan, W., Zeng, X., Han, Y., Liang, Q., Huang, R., Zhou, S., & Shu, J. (2025). Jarosite residues recycling by slurry electrolysis: Iron recovery and detoxification in one step. *Process Safety and Environmental Protection*, *195*, Article 106757. https://doi.org/10.1016/j.psep.2025.01.011 DOI 10.1016/j.psep.2025.01.011
87. Wang, R., Yan, Q., Su, P., Shu, J., Chen, M., Xiao, Z., Han, Y., & Cheng, Z. (2020). Metal mobility and toxicity of zinc hydrometallurgical residues. *Process Safety and Environmental Protection*, *144*, 366–371. https://doi.org/10.1016/j.psep.2020.07.042 DOI 10.1016/j.psep.2020.07.042
88. Wang, Y., Yang, H., Zhang, G., Kang, J., & Wang, C. (2020). Comprehensive recovery and recycle of jarosite residues from zinc hydrometallurgy. *Chemical Engineering Journal Advances*, *3*, Article 100023. https://doi.org/10.1016/j.ceja.2020.100023 DOI 10.1016/j.ceja.2020.100023.
89. Soe, K. M., Ruan, R., Jia, Y., Tan, Q., Wang, Z., Shi, J., Zhong, C., & Sun, H. (2021). Influence of jarosite precipitation on iron balance in heap bioleaching at Monywa copper mine. *Journal of Mining Institute*, *247*, 102–113. https://doi.org/10.31897/PMI.2020.1.11
90. Xing, Y., Wei, C., Deng, Z., Li, X., & Li, M. (2024). Controllable mechanism of hazardous jarosite transformation into recyclable hematite in the leaching solution of secondary zinc oxide powder. *Scientific Reports*, *14*, Article 24490. https://doi.org/10.1038/s41598-024-75857-5
91. Xu, C., Xie, Q., Xu, F., Zhou, Y., Wang, H., Chen, T., & Peng, S. (2021). Preparation of monoclinic pyrrhotite by thermal decomposition of jarosite residues and its heavy metal removal performance. *Minerals*, *11*(3), Article 267. https://doi.org/10.3390/min11030267
92. Xu, W., Yao, J., Liu, Z., Jiang, J., Xiao, S., & Li, Y. (2025). Amorphous porous $FePO_4$/reduced graphene oxide nanocomposite cathode material prepared from the leaching solution of jarosite residue with excellent lithium/sodium storage performance. *Journal of Power Sources*, *632*, Article 236401. https://doi.org/10.1016/j.jpowsour.2025.236401
93. Yang, Y., Chen, S., Wang, B., Wen, X., Li, H., & Zeng, R. J. (2020). Effect of ferric ions on the anaerobic bio-dissolution of jarosites by *Acidithiobacillus ferrooxidans*. *Science of the Total Environment*, *710*, Article 136334. https://doi.org/10.1016/j.scitotenv.2019.136334
94. Yu, X., Chen, Y., Zhong, W., Liu, X., Zhang, W., & Lin, Z. (2026). Kinetics-controlled lattice relaxation enables selective lead extraction from hazardous jarosite waste. *Chemical Engineering Journal*, Article 179771. Advance online publication. https://doi.org/10.1016/j.cej.2026.179771
95. Zeng, Y., Zhang, W., Wu, J., Wei, Y., Ke, Y., Shi, M., Yan, X., & Lin, Z. (2023). Simultaneous recovery of Fe_2O_3 and $PbCl_2$ from hazardous jarosite residues via hydrothermal phase transformation with NaCl. *Hydrometallurgy*, *221*, Article 106150. https://doi.org/10.1016/j.hydromet.2023.106150

96. Zhang, T., Zhang, K., Ding, C., Liu, Q., Liu, W., & Shi, Y. (2025). Pb alleviates As mobilization during the biological reductive dissolution of Pb–As jarosite. *Environmental Pollution, 366*, Article 125516. https://doi.org/10.1016/j.envpol.2024.125516
97. Zhao, T., Yang, H., Lin, D., Li, J., Zhang, S., Li, G., & Sun, Q. (2026). Efficient recovery of Fe, Pb and Zn from jarosite residues via reduction roasting and in-situ sulfidation: CRITIC-weighted response surface optimization, mechanism and engineering potential. *Process Safety and Environmental Protection, 216*, Article 109321. https://doi.org/10.1016/j.psep.2026.109321
98. Zhao, T., Yang, H., Lin, D., Zhang, S., Sun, Q., & Li, G. (2026). Recovery of Fe, Pb, and Zn from jarosite residues and realization of clean production through reduction roasting–grinding magnetic separation–tailings backfilling: Effects, mechanisms, and applications. *Journal of Cleaner Production, 553*, Article 148019. https://doi.org/10.1016/j.jclepro.2026.148019
99. Zhou, Q., Pan, J., Zhu, D., Yang, C., Guo, Z., Li, S., &Xu, X. (2025). New process for efficient separation and comprehensive recovery of valuable metals from jarosite residues. *Metals, 15*(2), Article 171. https://doi.org/10.3390/met15020171
100. Zhou, S., Han, Y., Huang, R., Huang, Y., Dong, Q., Gang, H., Qin, J., Yu, X., Zeng, X., Cao, W., Wang, J., Chen, S., Wang, R., & Chen, M. (2024). Making waste profitable: Efficient recovery of metallic iron from jarosite residues. *Chinese Journal of Chemical Engineering, 71*(7), 66–76. https://doi.org/10.1016/j.cjche.2024.04.004
101. Zhou, X., Chen, Y., Tan, F., An, J., & Yang, W. (2024). Selective removal of iron from sulfuric acid leaching solution of aerospace magnetic material scraps by jarosite process. *Waste Management, 188*, 107–116. https://doi.org/10.1016/j.wasman.2024.08.007
102. Zulhan, Z., Adzana, Z., Munawaroh, M., Yusro, A. H., Christian, J. D., Saputri, A. D., & Hidayat, T. (2023). Sulfur removal and iron extraction from natrojarosite residue of laterite nickel ore processing by reduction roasting. *Metals, 13*(1), Article 52. https://doi.org/10.3390/met13010052